

Dedicated to the people who lost their lives and injured by
the 2008 Wenchuan Earthquake

A RECONNAISSANCE REPORT
ON
2008 WENCHUAN EARTHQUAKE*

Japan Society of Civil Engineers
Earthquake Engineering Committee
Earthquake Disaster Investigation Sub-Committee

May 19, 2008

* This report has been compiled and edited by Ömer Aydan (Tokai University)

CONTENT

1 INTRODUCTION	3
2 GEOGRAPHY	5
3 GEOLOGY AND TECTONICS	8
4 SEISMICITY	13
5 CHARACTERISTICS OF THE EARTHQUAKE AND FAULTING	15
6 STRONG MOTIONS**	20
7 CASUALTIES	23
8 DAMAGE TO STRUCTURES	24
8.1 Bridges**	24
8.2 Damage to Roadways and Railways	33
8.3 Damage to Tunnels	37
8.4 Damage to Pylons and Poles	42
8.5 Dams and Powerhouses	44
8.6 Industrial Facilities	
9 SLOPE FAILURES AND QUAKE LAKES	48
9.1 Slope failures	48
9.2 Mitigation Measures	57
9.3 Quake lakes	58
10 LIQUEFACTION AND LATERAL SPREADING	63
11 DAMAGE TO BUILDINGS	68
11.1 Damage to Masonry Buildings	68
11.2 Reinforced Concrete Buildings	71
11.3 Faulting-induced Damage to Buildings	77
11.4 Landslides and rock fall-induced damage to buildings	79
12 CONCLUSIONS	83
REFERENCES	83

* *See the article by Kawashima et al. on strong motions and bridges

1 INTRODUCTION

An earthquake with an estimated magnitude of 7.9 struck Sichuan Province of China Sichuan Province at 2:28 p.m. local time (06:28 UTC) on May 12, 2008. The quake was felt throughout much of China, as well as parts of Taiwan, Thailand, and Vietnam. The confirmed casualties are more than 79000. The earthquake caused widespread damage to buildings, transportation facilities, industrial plants and large-scale slope failures in the earthquake-affected area.

The earthquake occurred at the well-known and well-studied Longmen Shan Fault Zone by thrust faulting with dextral component. Preliminary analyses indicate that the rupture process has activated a 300km long fault section. However, there are two successive rupturing processes. The first rupturing is associated with thrust faulting with slight dextral movement while the second rupturing process indicates almost pure dextral movement and it is about 40km away from the NE end of the first rupture zone.

The strong motion records are not available to scientific world yet. However, the preliminary estimations indicate that the ground motions are high in epicentral area. The maximum ground acceleration and velocity are expected to exceed 1G and 100 kine.

A huge number of reinforced concrete buildings collapsed in the epicentral area. The preliminary reports indicate that 5 million people are homeless. The collapse of structures was mainly associated with high ground motions together with their low earthquake resistance. Furthermore, permanent ground deformation induced by landslides as well as relative motion of the earthquake fault also played a major role in the widespread damage.

The information is still lacking and most of sources are not accessible through international communities interested with the scientific and engineering aspects of this earthquake. This preliminary report is prepared with a sole purpose of providing an overall view of various aspects of the earthquake, which may be usefull to the researchers and investigators interested and/or involved with the Wenchuan earthquake.

Table 1.1: Members of the first dispatched team by JSCE together collaborating members from AIJ and JSI

Member	Affiliation
Masanori Hamada	Waseda University
K. Kawashima	Tokyo Institute of Technology
Ömer AYDAN	Tokai University
K. Honma	NEXCO
K. Ohkubo	NEXCO
J. Itoh	SAVE-EARTH
S. Wu	Oyo Corporation

2 GEOGRAPHY

The earthquake occurred in Sichuan province of China (Figure 2.1). Chengdu with a population of 10 million is the largest city and it is the provincial capital of Sichuan. The epicenter of the earthquake is in Wenchuan County, which is about 90km away from Chengdu. The area affected area is mountainous and the elevation of mountains reaches the height of 5000m (Figure 2.2). The earthquake caused wide-spread structural damage as well as geotechnical damage in Wenchuan, Yingxiu, Maowen, Beichuan, Shifang, Hanwang, Mianyang, Dujiangyan, Deyang, Mianzhu (Figure 2.3).



Figure 2.1. Location of the epicenter of the Wenchuan earthquake in Shichuan Province

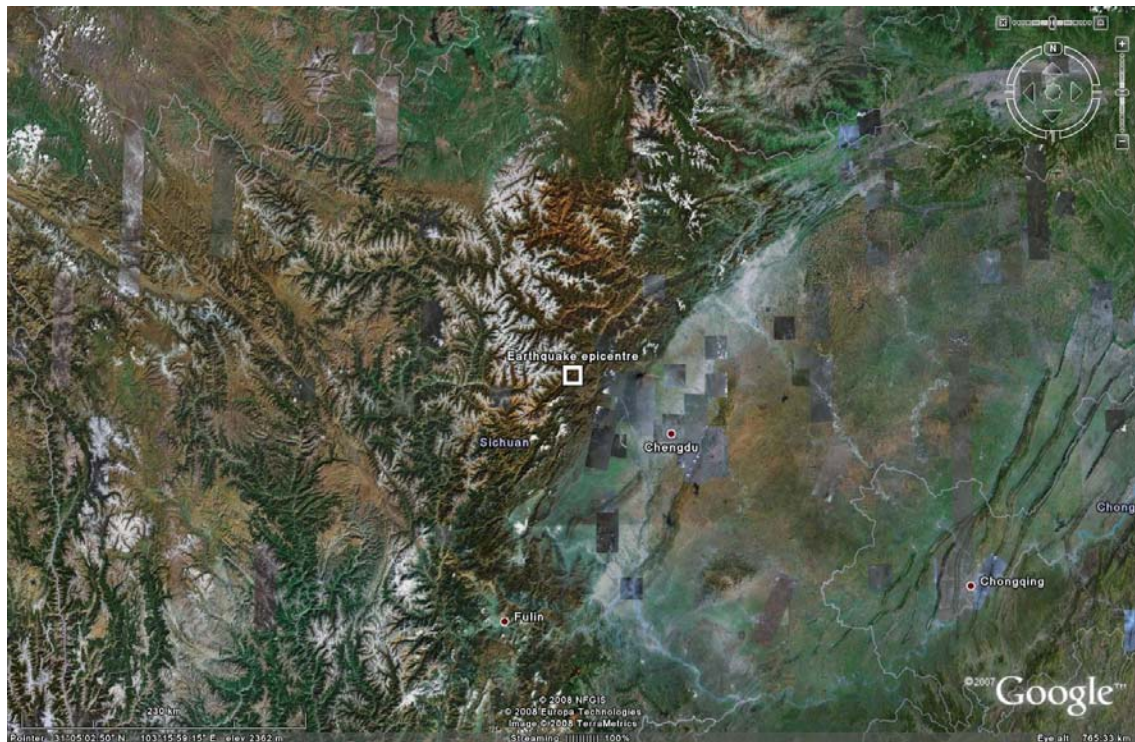


Figure 2.2. Topography and satellite view of Sichuan Province (from Google earth)

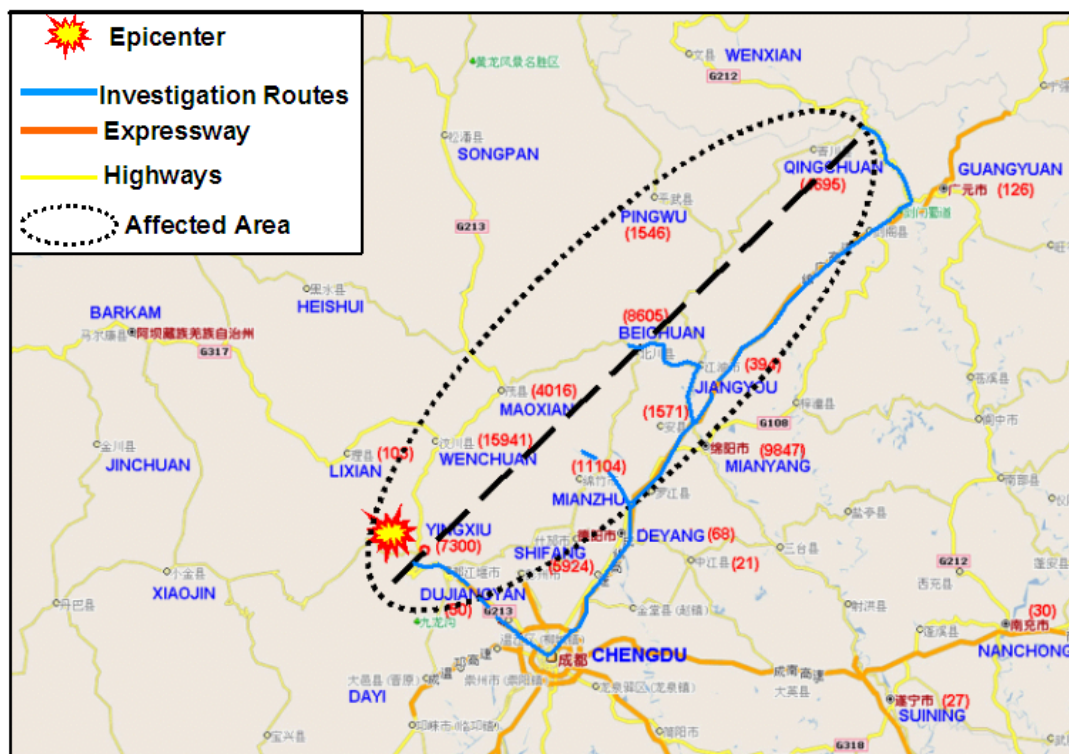


Figure 2.3. Major cities and towns affected by the earthquake (base map from Google)

3 GEOLOGY AND TECTONICS

3.1 Geology

The section on the geology and tectonics of Sichuan province is based on a series of publications by Burchfiel et al. (1995), Şengör et al. (1993), and Meng et al. (2006). The geology of the Longmen Shan region is divided into four distinct tectonostratigraphic packages. From oldest to youngest, these include (1) crystalline basement rocks of the Yangtze craton, (2) Neoproterozoic-Permian passive margin sediments, (3) Triassic flysch of the Songpan-Garze terrane, and (4) Mesozoic-Cenozoic terrestrial sediments in the Sichuan Basin (Figure 3.1). These packages are juxtaposed across a series of structures, collectively termed the Longmen Shan Thrust Belt (Burchfiel et al., 1995).

Crystalline rocks of the Yangtze craton are exposed in a belt of basement massifs adjacent to the southwest corner of the Sichuan Basin. The massifs consist of quartzofeldspathic gneisses and associated granitoids that are thought to be Precambrian. They are structurally overlain by a parautochthonous passive margin sequence, and thus assumed to represent the basement of the Yangtze craton. The passive margin sequence itself consists primarily of shallow water marine rocks of Neoproterozoic (Sinian) to Permian age. Permian carbonates generally grade into deep-water deposits of the Songpan-Garze terrane, a 500,000 km² region of vertically dipping, isoclinally folded Triassic flysch and graywacke that may represent incomplete closure of a Paleotethyan ocean basin.

All three tectonostratigraphic packages were deformed during Mesozoic time as evident in a series of east directed thrusts that place the Neoproterozoic-Triassic passive margin sequence atop the craton. The thrust belt trends northeast and merges with the E-W trending Qinling orogen north of the Sichuan Basin. Northwest trending folds within the Songpan-Garze wrap into parallelism with the western edge of the Longmen Shan thrust belt, and likely indicate that the thrust belt had a significant sinistral component during Mesozoic transpressional deformation (Burchfiel et al., 1995).

Substantial metamorphism and plutonism accompanied Mesozoic deformation in the Longmen Shan region. Metamorphic grade of the passive margin sequence ranges from negligible to lower amphibolite and generally increases toward the hinterland. Metamorphism was accompanied by emplacement of a suite of Mesozoic plutons (generally granodiorite to monzonite) into the Triassic flysch northwest of the thrust belt. These plutons are generally macroscopically undeformed and cut across isoclinal, upright folds within the flysch. Contact metamorphic mineral assemblages from the flysch adjacent to the plutons include andalusite and cordierite. Contact metamorphic

minerals overgrow regional fabrics within the flysch, and, combined with the undeformed nature of the granitoids themselves.

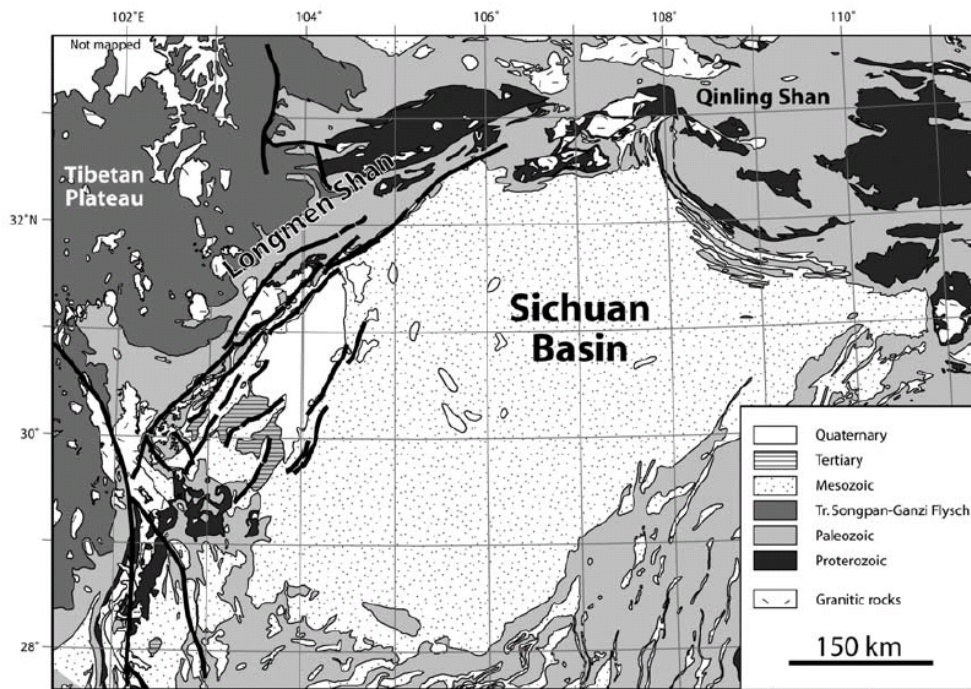


Figure 3.1 Geology of Sichuan Basin and its close vicinity (Densmore et al. 2007)

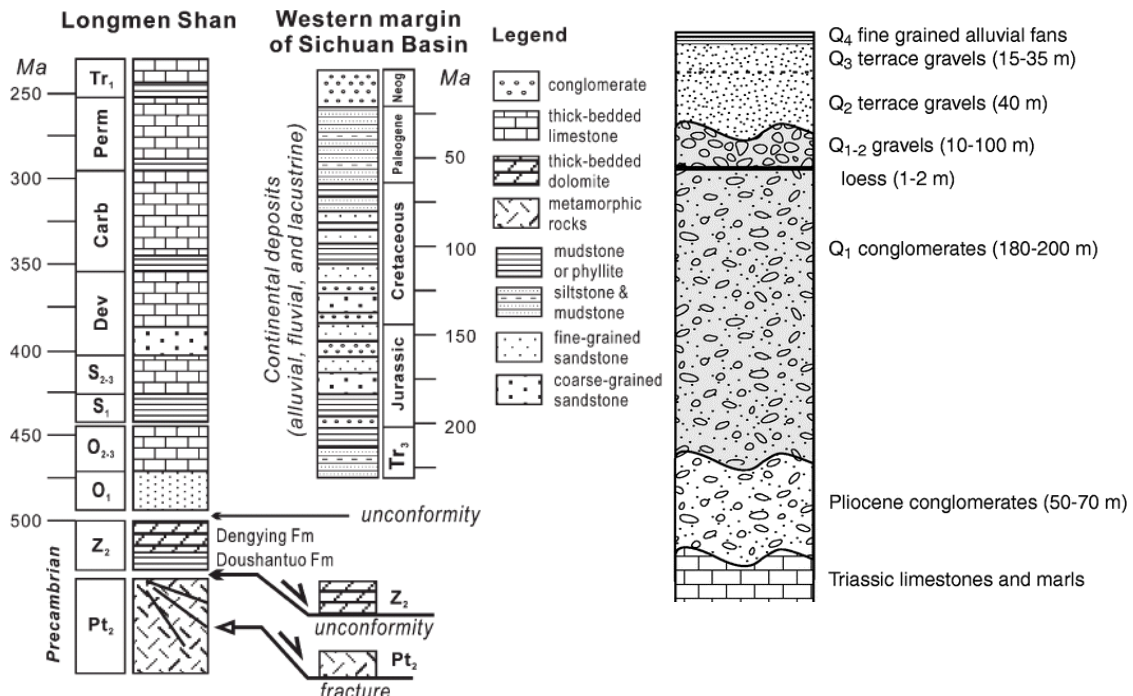


Figure 3.2. Simplified stratigraphy of Sichuan Basin and its close vicinity (modified from Meng et al. 2006 and Densmore et al., 2007).

3.2 Tectonics

The regional tectonics greatly influenced by the steady northward push of the Indian tectonic plate into the Eurasian plate. The two plates converge with a velocity of about 50 millimeters a year, lifting up the Tibetan Plateau (Figure 3.3). As the plates collide, the crust underlying the Tibetan Plateau moves and encounters strong crust under the Sichuan Basin. Tapponier and Molnar (1976) studied the regional tectonics and they reported a clay model test in which a rigid plate representing the Indian plate is pushed into the soft clay layer (Figure 3.4). In spite of the simplicity of the model, it could capture overall tectonic pattern and can explain the crustal movements.

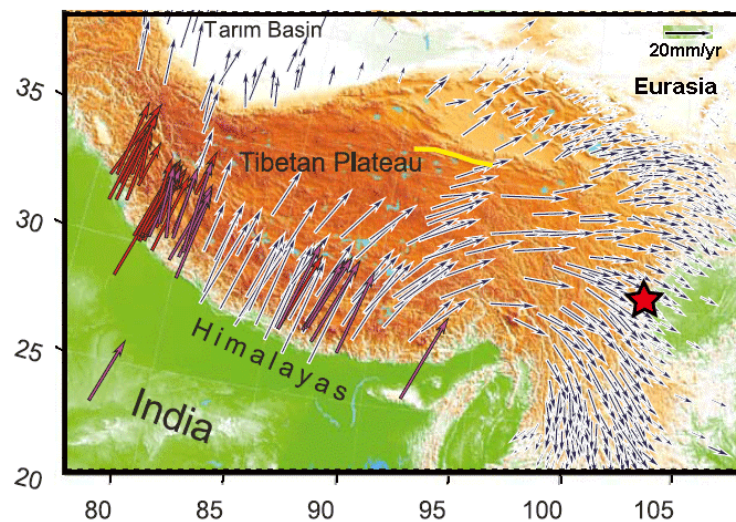


Figure 3.3. Annual crustal deformation velocities obtained from GPS measurements (arranged from Gan et al. 2007)

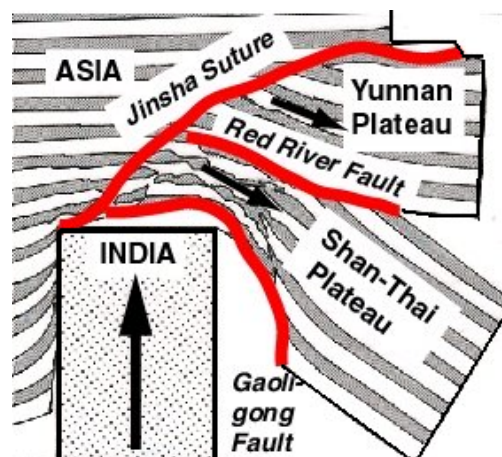


Figure 3.4. The application of the clay model by Tapponier and Molnar (1976) to Central and South-east Asia.

Figure 3.5 shows the major regional tectonic features. The Tibetan platform pushed by the Indian plate moves northward and accommodates the deformation through some strike-slip faulting along Altın Dağ (Altyn Dagh), Tanrı Dağ (Tien-shan), Karakorum, Jiali-Red River, Xian-Shui-He, Haiyuan faults and restricted by Longmen-shan fault. This area experienced very large earthquakes such as 2001 M7.8 Kunlun earthquake, 1997 M7.8 Manyi earthquake, 1977 M6.7 Songpan-Huya earthquake. 2008 M8.0 Wenchuan earthquake occurred along Longmen-shan fault zone.

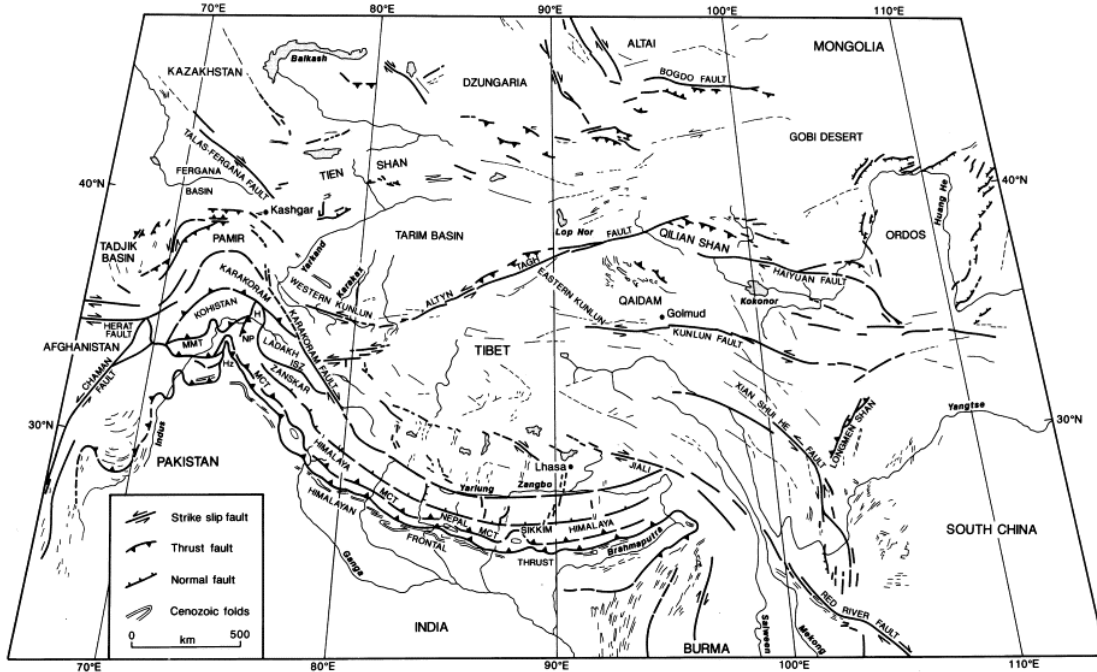


Figure 3.5. Major regional tectonic features

There are many quaternary and Holocene-aged strike-slip faults in the Longmen Shan region, the boundary between the eastern Tibetan plateau and the Sichuan basin in west-central China (Figure 3.6). Active faults within the mountainous region include the N to NNE-trending Min Jiang and Huya faults and the ENE-trending Maowen-Wenchuan, Beichuan and Pengguan faults (Densmore et al. 2007). The latter are exposed for hundreds of kilometers within the Longmen Shan proper. Less well-known but probably equally significant is the NNE-trending Dayi fault, which lies at and partly defines the edge of the Chengdu basin, the western sub-basin of the Sichuan Basin. The Huya Valley fault marks the eastern boundary of the N-S trending Min Shan, and is generally mapped as a west-dipping thrust. Observations and inspection of aerial photographs over a distance of ~30 km reveals a prominent N to NNW trending fault that offsets a channel sinistrally by ~100m. The Beichuan fault, near Beichuan, comprises three distinct ENE-trending en echelon segments. Channel and ridge offsets

show clear evidence for sinistral displacement. The fault is well expressed across the youngest terrace ~4m above the modern river and likely of Holocene age. A minor thrust component is visible along part of the fault, but the overall expression is predominantly strike-slip.

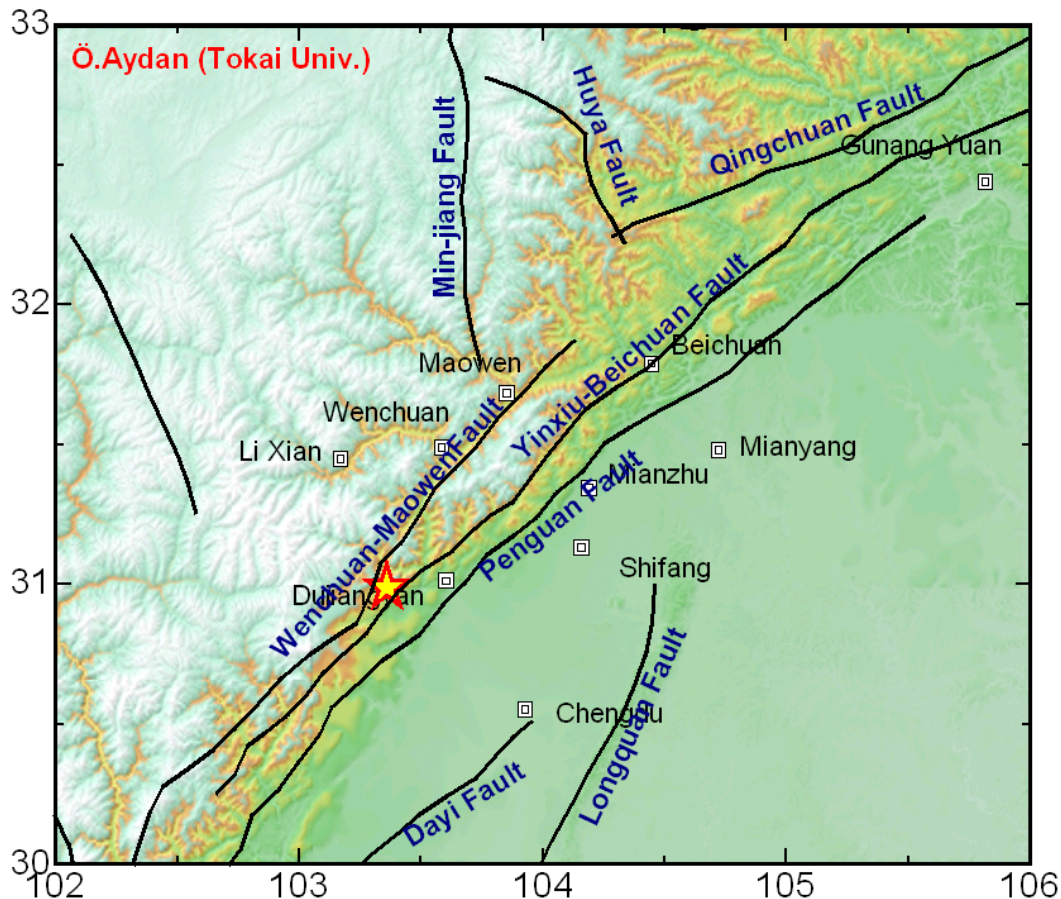


Figure 3.6. Major faults in Longmen-shan fault zone

The Pengguan fault is observed immediately north of An Xian where it crosses a Holocene floodplain and is expressed as a 2m high north-up scarp trending ENE. A sag pond has developed in response to a right-bend, indicating dextral displacement. We observed the same fault 170 km farther southwest, near Shuanghe. Prominent 15m-high pressure and shutter ridges, offset channels, and linear scarps mark the fault here across both low and high fluvial terraces. Displacement is unequivocally dextral and predominantly strike-slip. The Dayi fault, 5 km north of Dayi, is expressed by at least three dextral channel offsets and associated shutter ridges. Exposures of the Pliocene-Quaternary Dayi conglomerate show easterly verging folds and minor fault zones that may reflect active deformation. The geomorphic expression of these faults suggests to us that they young, or slip rates increase, toward the Sichuan Basin. These

observations are consistent with those from our earlier reconnaissance fieldwork and taken together show that deformation of the Longmen Shan is currently dominated by crustal-scale conjugate strike-slip faults. The author also did some measurements on fault outcrops at Longxi, Shoujiang and Juijiaya sites along Yingxiu-Beichuan fault zone. The results of orientation measurements are given in Table 3.2 and their focal mechanisms are shown in Figure 3.7.

Table 3.1. Characteristics of major faults (compiled from Chen and Wilson, 1995 and Densmore et al. 2007)

Fault Name	Dip Direction	Dip	Rake
Wenchuan-Maowen	310-330(Av:320)	50-70(Av:60)	240-260(Av:250)
Yingxiu-Beichuan	305-315(Av:310)	50-70(Av:60)	240-265/183-220
Penguan Fault	310		240-250(Av:245)
Dayi Fault	320-330	60	

Table 3.2. Measurements on the orientation and striation of several fault outcrops

Locality	Latitude	Longitude	Dip Direction	Dip	Rake	Comment
Longxi T.	31.0259	103.5395	18	63	255	SE Entrance
Shoujiang B.	30.9773	103.4605	322	50	300 240	Old stria New stria
Juijiaya T.	32.4546	105.2419	310	64	250	South Entrance

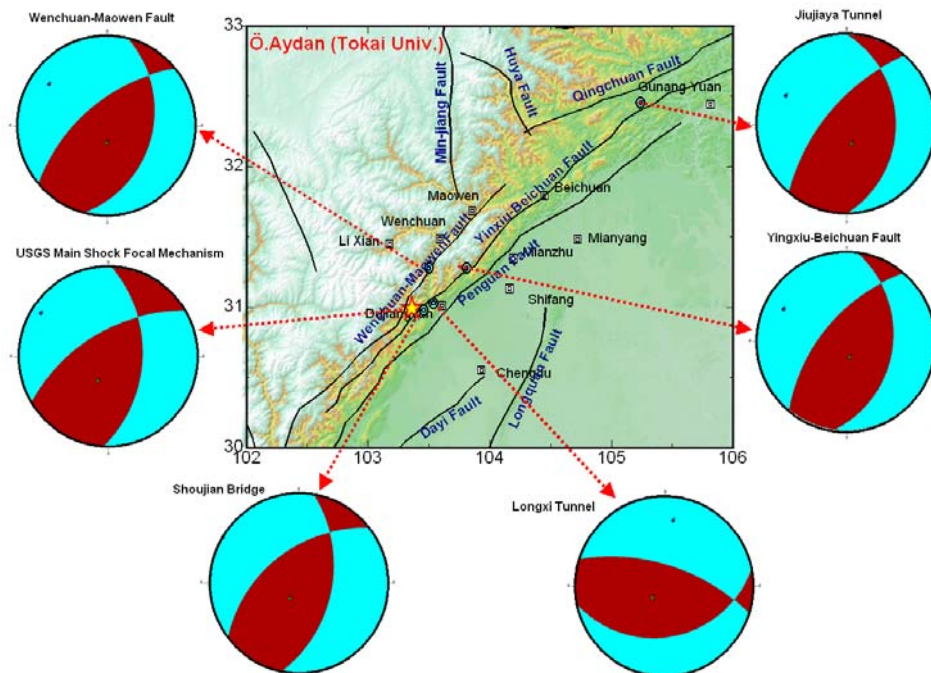


Figure 3.7. Inferred focal mechanism of the fault outcrops

4 SEISMICITY

Figure 4.1 shows the seismicity of the region using the USGS database together with major historical events reported. The historical seismicity data is compiled from various sources (Lu et al. 2004; Yang et al. 2005; China Earthquake Administration 2008). As noted from Figure 4.1, the seismicity between 1973 and 2008 before the main shock occurred along the well-known faults in the domain bounded by Latitudes 30-33 and Longitudes 102-106. However, there is no earthquake with magnitude greater than 7 within the Longmenshan fault zone. Figure 4.2 shows the focal plane solutions of some past earthquakes compiled from data released by Yang et al. 2005 and USGS. The focal plane solutions of the earthquakes in Longmenshan fault zone indicate that earthquakes are due to either thrust faulting with dextral component or pure dextral slip.

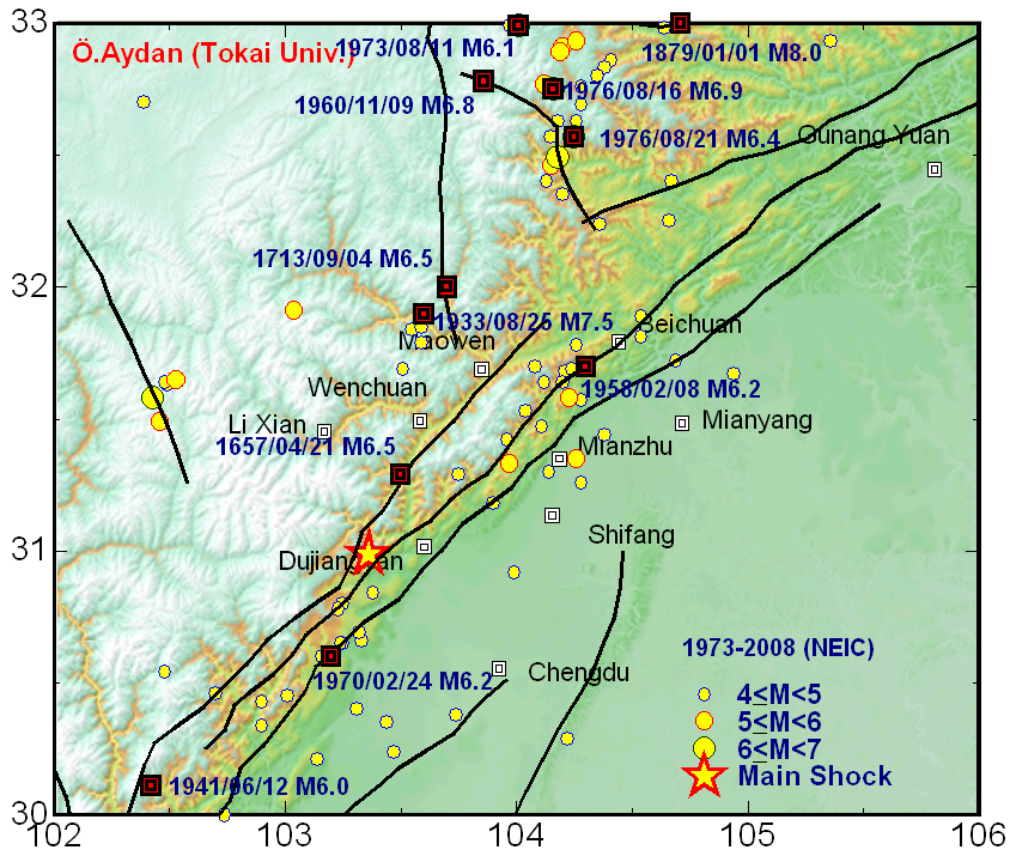


Figure 4.1. Historical and modern seismicity of the earthquake affected region

An statistical anaysis of the seismicity of the region bounded by Latitudes 30-33 and Longitudes 102-106 has been carried out and the results are shown in Figure 4.3. The fitted Gutenberg-Richter relation is also shown in the same figure. As noted from the figure and b-value of the Gutenberg-Richter relation, the seismicity of the region is not high.

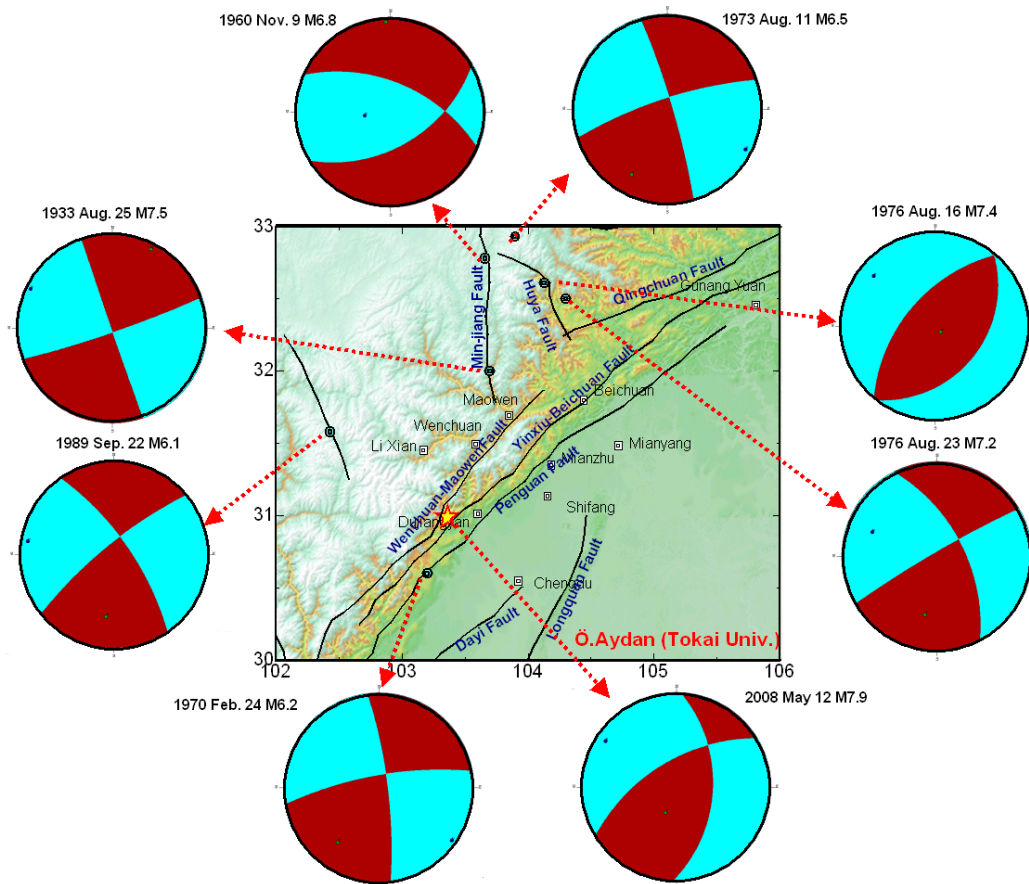


Figure 4.2. Focal plane solutions of some earthquakes

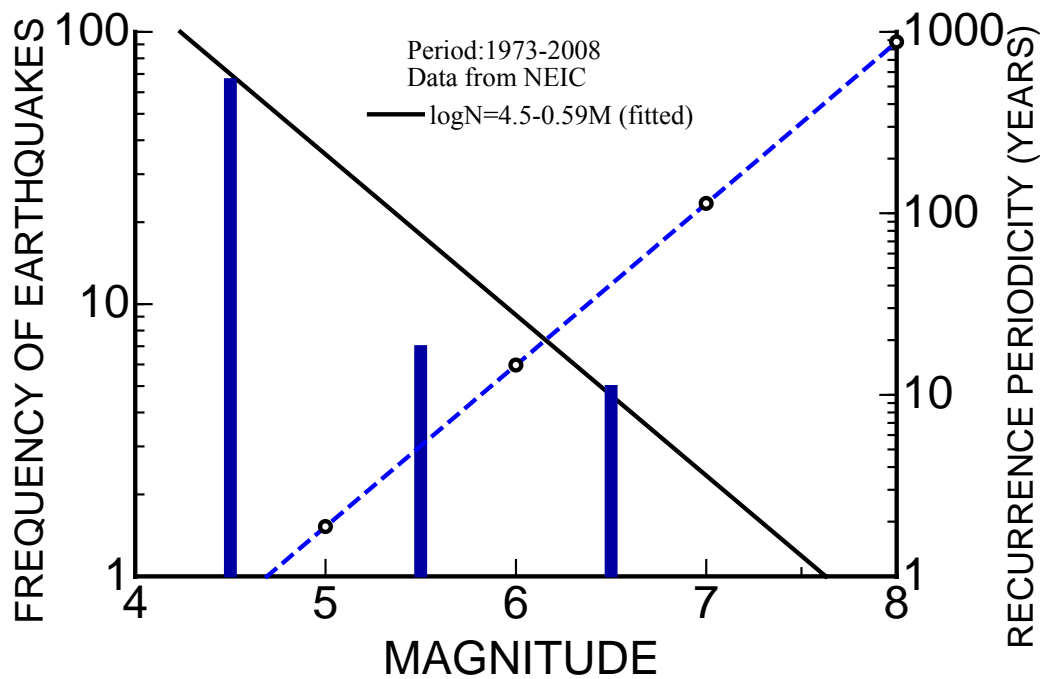


Figure 4.3. Gutenberg-Richter relations for the earthquake affected area

5 CHARACTERISTICS OF THE EARTHQUAKE AND FAULTING

The fundamental parameters of the May. 12, 2008 earthquake estimated by various institutes worldwide and they are listed in Table 5.1. Furthermore, the focal mechanism solutions are shown in Figure 5.1. Although there are some differences among the parameters of the earthquake estimated by various institutes, the all solutions indicate thrust faulting with a slight lateral component. As two fault planes are obtained from these solutions, the causative fault should be inferred from additional observations and seismic data. In view of the regional tectonics, after-shock activity, the fault plane dipping to NW should be the causative fault. If NW dipping fault is taken as the causative fault, then lateral strike-slip component of the faulting implies dextral motion of the fault.

Table 5.1: Parameters of the earthquake estimated by different institutes

Institute	Latitude	Longitude	Depth (km)	Magnitude	Strike	Dip	Rake
HARVARD	31.49	104.11	12	M _w =7.9	NP1 229° NP2 352°	33° 70°	141° 63°
USGS	31.969	103.186	16	M _w =7.9	NP1 239° NP2 2°	59° 47°	128° 45°
IGP-CEA	31.021	103.367	10	M _s =8.0 M _w =8.3	NP1 229° NP2 7°	43° 55°	123° 63°
Nishimura-Yagi	-	-	10	M _w =7.9	NP1 229°	33°	146°
Yamanaka-NGY	-	-	11	M _w =7.8	NP1 230°	30°	120°

Fault rupture propagation was inferred by various institutes and some of them listed in Table 5.2. The first computational results were released by Nishimura and Yagi of Tsukuba University (2008), which were followed by the others (Figure 5.2). Nishimura-Yagi (2008) and Yamanaka (2008) pointed out that a 120km fault ruptured with a dominant thrust mode first, and it was followed by almost strike-slip faulting by a 10 second delay. Although the overall rupture length seems to be about 300km long, the earthquake is a results of two fault segments successively. Furthermore, it was pointed out that there is 50-100km long gap between two ruptured fault segments.

The solutions estimated that maximum slip should be ranging between 6.6 and 13m. The empirical relations proposed by Aydan (2007) and Wells & Coppersmith(1994)

infer the relative slip to be 7-8.9 m and , 2.9-13.3 m, respectively by using the moment magnitude of 7.9 for thrust and strike-slip faulting modes.

The estimated dip angle of the fault ranges between 30 and 59°. If the dip angle is taken as 30°, the net-slip would range between 5 and 7.5 m for pure thrust mode. On the other hand, if the dip angle is taken as 59°, the net-slip would range between 2.9 and 3.5 m for pure thrust mode. The estimations by Nishimura-Yagi (2008), Yamanaka (2008) and Aydan (this study, 2008) are close to those measured at earthquake fault outcrops. Nevertheless, the inferred slips by ERI-TU and IGP-CEA are somewhat overestimations.

Table 5.2 Rupture and slip characteristics of the earthquake fault

Reference	Magnitude	Length(km)	Slip(m)	Area(km ²)	Vr(km/s)	Tr (s)
Nishimura-Yagi	7.9	350	6.60	350x70	3.2	120
Yamanaka-NGY	7.8	120+140	6.70	260x50		110
ERI-TU	7.9	320	13.00	320x40		100-120
JAMSTEC	8.0	320	9.30	320x30		110
IGP-CEA	8.3	300	12.00	300x45	3.1	
Aydan (thrust:tf)	Mw=7.9	150	7.00	150x24		77
Aydan (strike-slip:ssf)	Mw=7.9	230	8.87	230x24		79
Wells-Coppersmith(tf)	Mw=7.9	150	2.90	5600		
Wells-Coppersmith(ssf)	Mw=7.9	220	13.30	4980		

The Chinese Geological Survey Team (2008) surveyed the worst-hit areas of Yingxiu, Beichuan and Qingchuan, and investigated the surface ruptures. Observations of the ruptures ascertained that the causative structure of the earthquake was the Yingxiu-Beichuan fault in the north-central segment of the Longmenshan tectonic belt (Figure 5.3). Along the Yinxiu-Beichuan segment, rupture structures included road arching, mole tracks, push ridges and tensional fractures, which indicate eastward thrusting of the Yingxiu-Beichuan fault with vertical displacements of 2.5-3m, accompanied by a dextral strike-slip component. The co-seismic vertical displacements measured at Yingxiu Township and the seat of Beichuan County showed the same order of amplitude at several locations indicating that the upward movement of the fault ranges between 2.5 and 3 m.

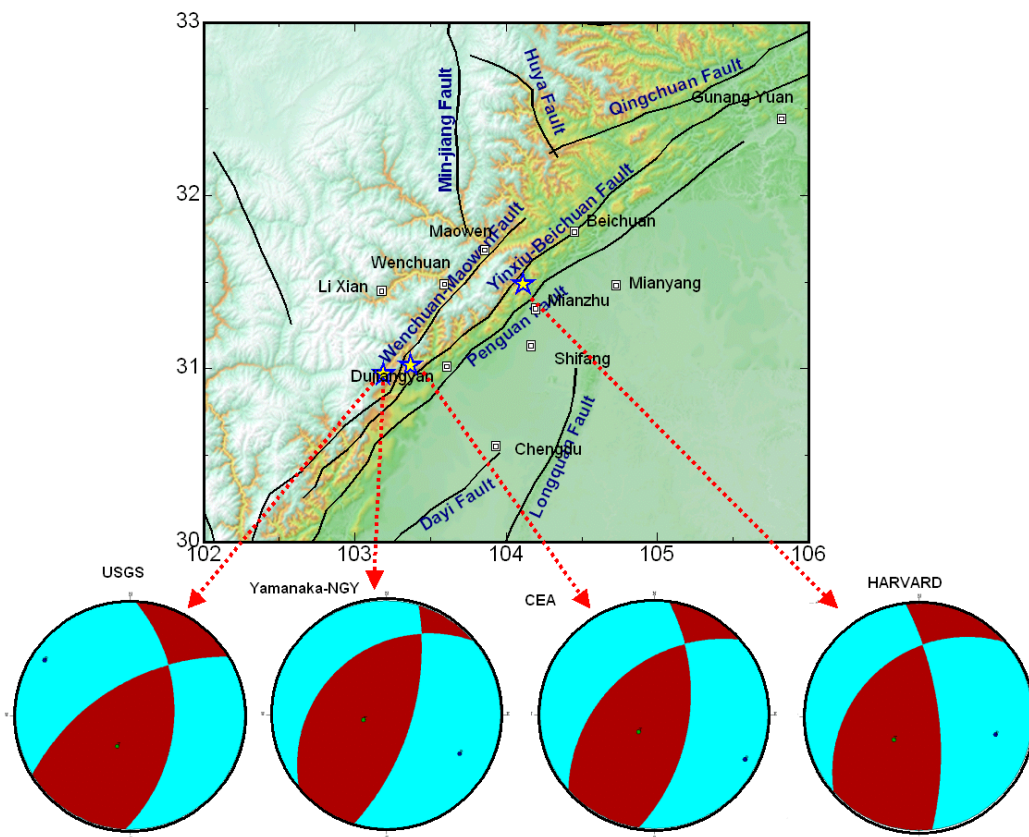
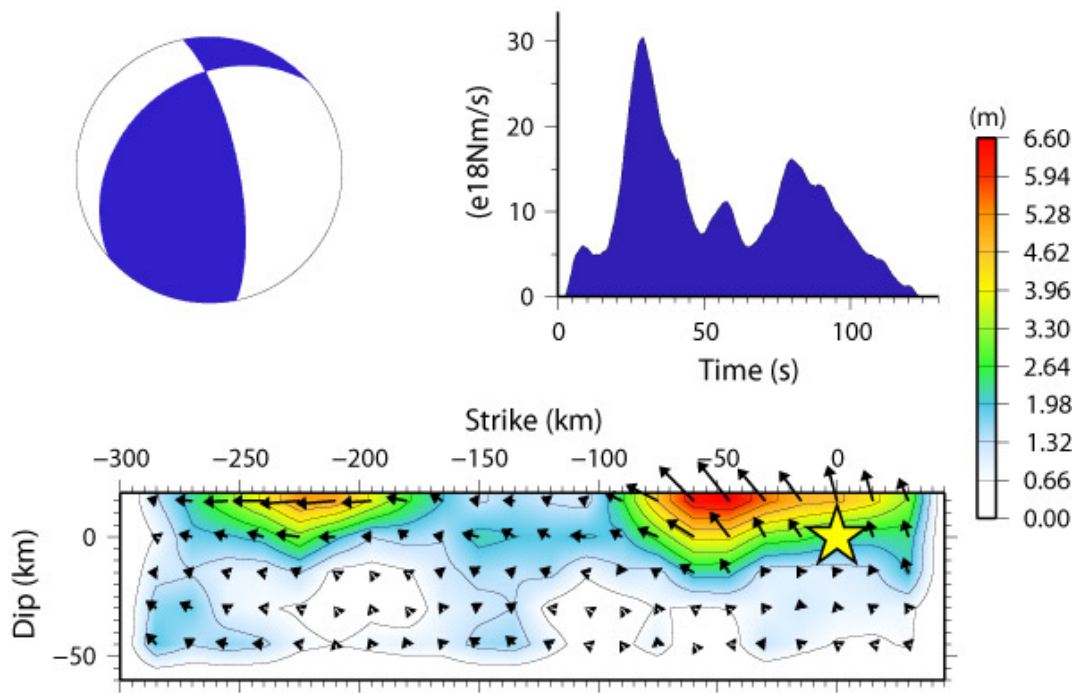


Figure 5.1. Illustration of epicenters and focal plane solutions by various institutes



Nishimura and Yagi (2008)

Figure 5.2. The slip distribution computed by Nishimura and Yagi (2008)



Figure 5.3. Surface ruptures in the earthquake affected area (from CAGS, 2008)

Japan Geographical Surveying Institute (2008) inferred the ground displacement using SAR method. The solutions by this institute indicated that the maximum ground displacements are upward on the hanging wall side of the fault (Figure 5.4). Nevertheless, the amplitude of inferences in the vicinity rupture zone could not be identified. The possible reasons may be extensive topographical changes resulting from slope failures as it often happens in thrust-type earthquakes such as the 1999 Chi-chi earthquake and 2005 Kashmir earthquake.

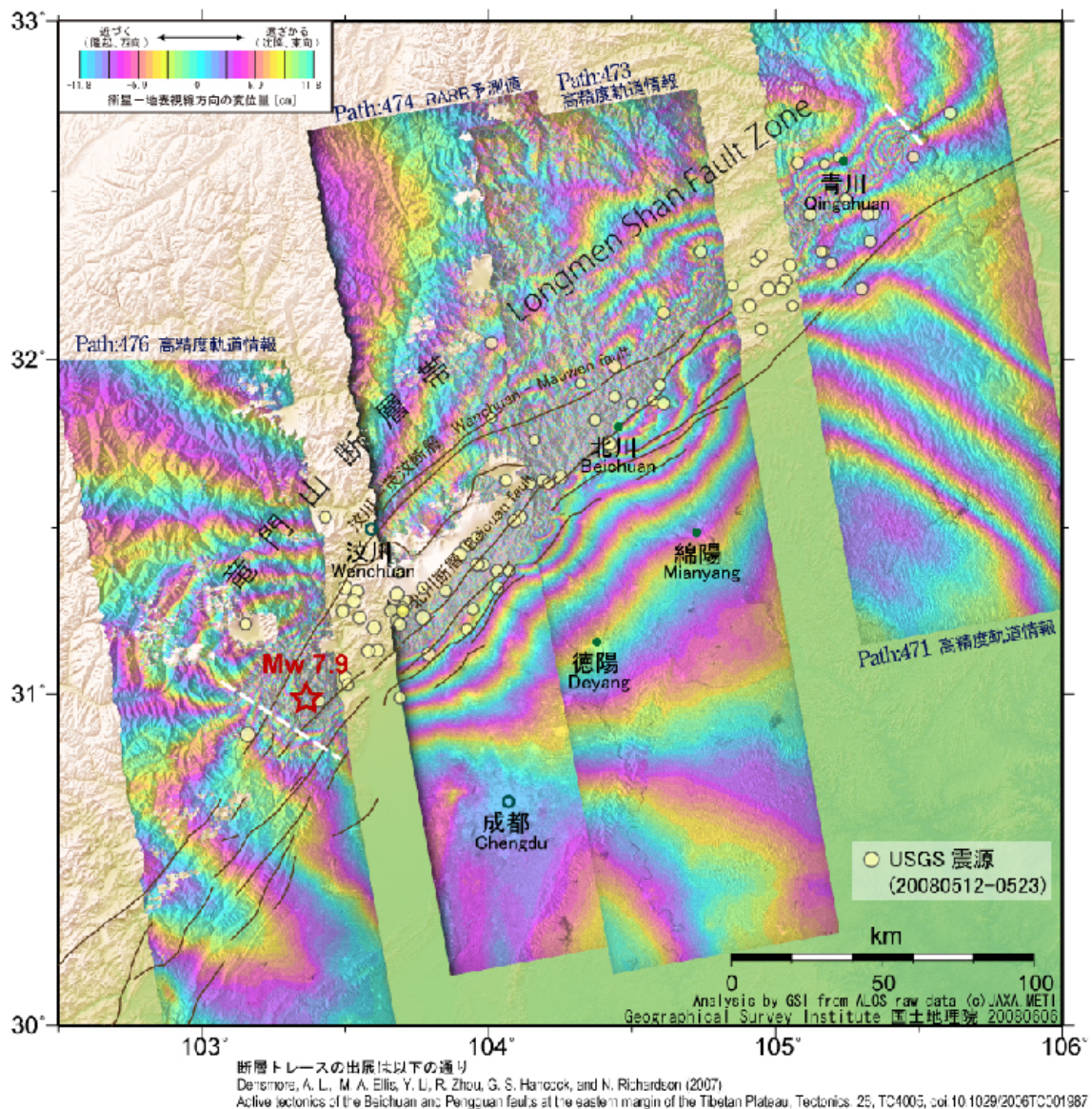


Figure 5.4. Contours of ground deformation inferred from SAR analysis (from JGS)

6 STRONG MOTIONS

There are several strong motions networks operated by different institutes in China. However, the digital data from strong motion networks are not available to the international earthquake engineering community yet. There are acceleration contour maps published by China Earthquake Data Center (CEDC, 2008). However, the value of contour lines are ineligible in the released figures. The available data through various sources are compiled and plotted in Figure 6.1 including the information released by China Earthquake Data Center. Some of records are shown in Figure 6.2. The maximum ground acceleration is more than 800 gals in the close vicinity of earthquake epicenter. The maximum acceleration was 2000 gal at the crest of Zipingpu dam. However, it should be that the maximum ground acceleration at the dam crest contains the amplification factor due to the dam body. As noted from this figure, the attenuation relations for intraplate earthquakes are not far below the reported measurements. The estimations by the attenuation relation proposed by Aydan and Ohta (2006) for interplate earthquakes somewhat closer to the reported measurements. Figure 6.3 shows the contours of maximum ground acceleration and velocity using the epicenter estimated HARVARD.

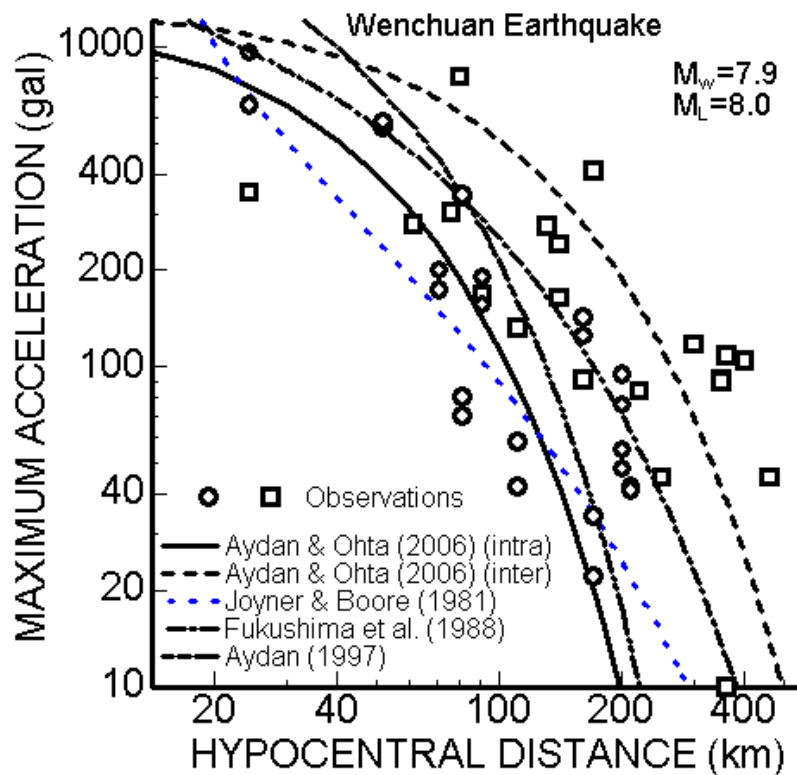
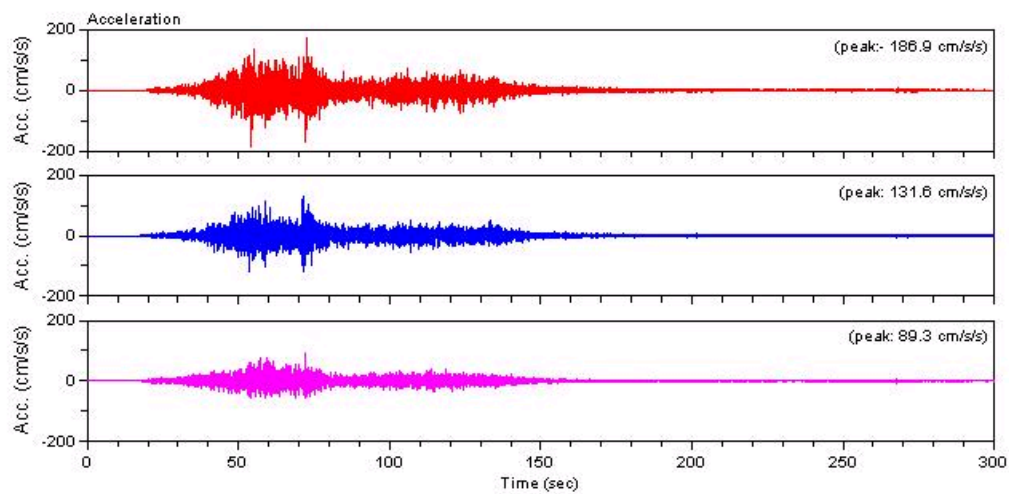
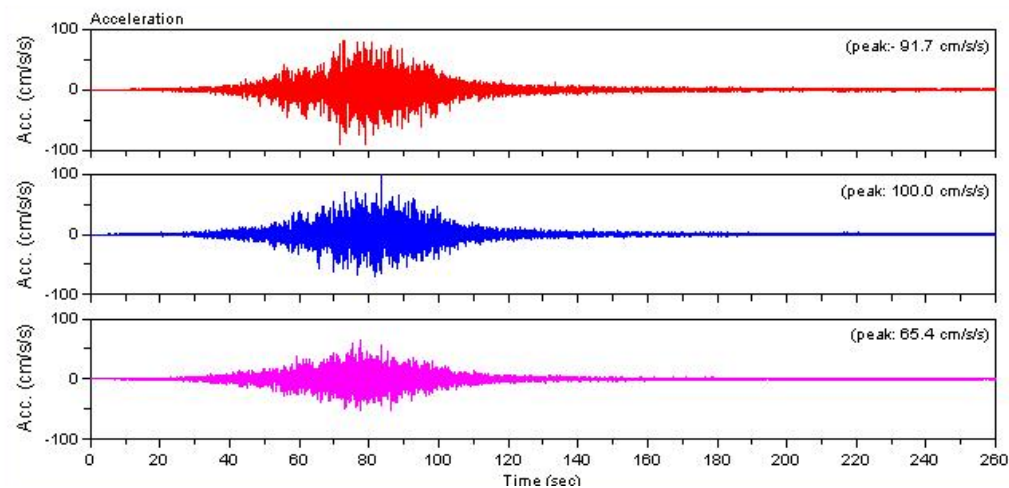


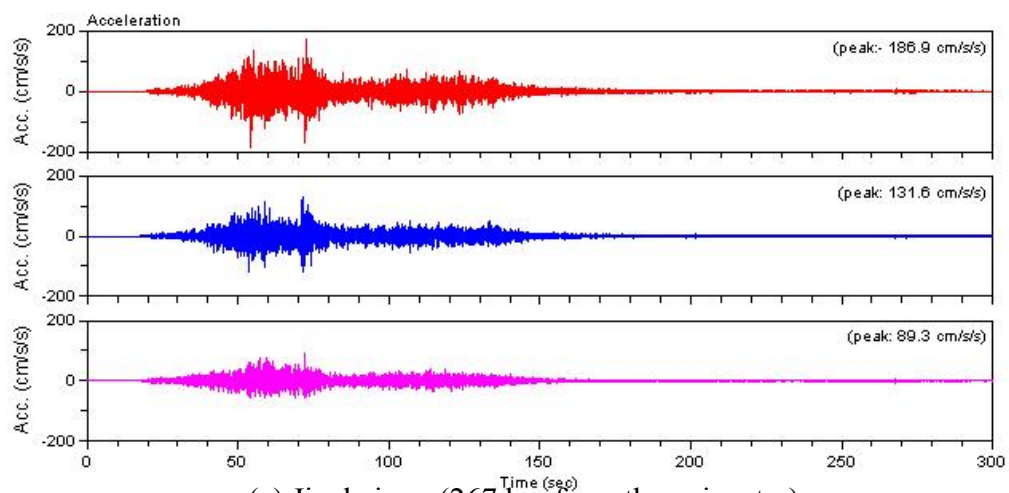
Figure 6.1 Comparison of observed maximum ground acceleration with some of empirical attenuation relations



(a) Songpan (168 km from the epicenter)



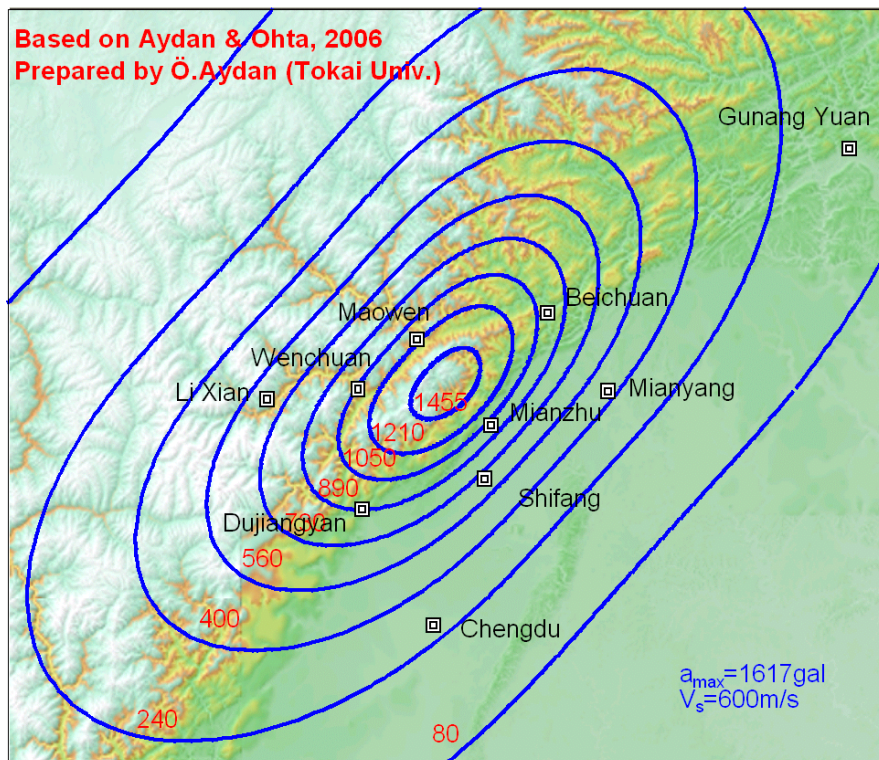
(b) Luding (177 km from the epicenter)



(c) Jiuzhaigou (267 km from the epicenter)

Figure 6.2. Acceleration records (from China Earthquake Data Center, 2008)

Maximum Ground Acceleration



Maximum Ground Velocity

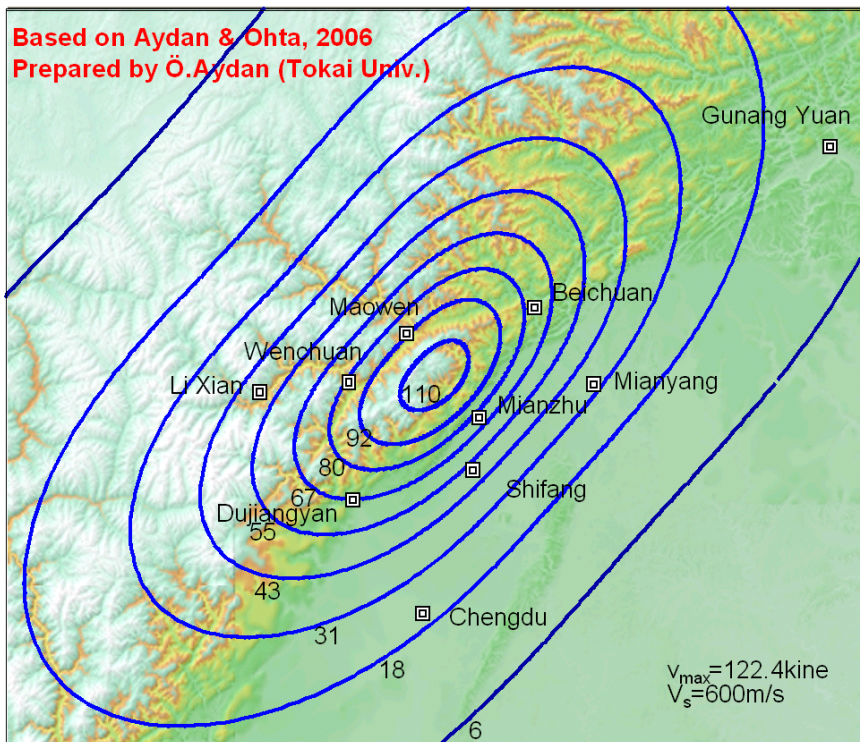


Figure 6.3. Estimated ground motion contours for Wenchuan earthquake using interplate attenuation relations

7 CASUALTIES

The number of casualties caused by this earthquake stands 69,188 as of June 29, 2008 according to the State Council Information Office. The number of the missing people is 18440. The number of the injured people is 374,177. Figure 7.1 shows the counties and cities together with the number of casualties. The number of casualties is shown in parenthesis. As noted from the figure, the highest casualties occurred in Yingxiu, Dujiangyan, Wenchuan, Beichuan, Mianzhu, Shifang and Qingchuan. These counties and cities are situated on a 270 long and 70km wide earthquake fault zone. About 5 million people have become homeless. As of June 29, 2008, 364000 temporary houses are built.

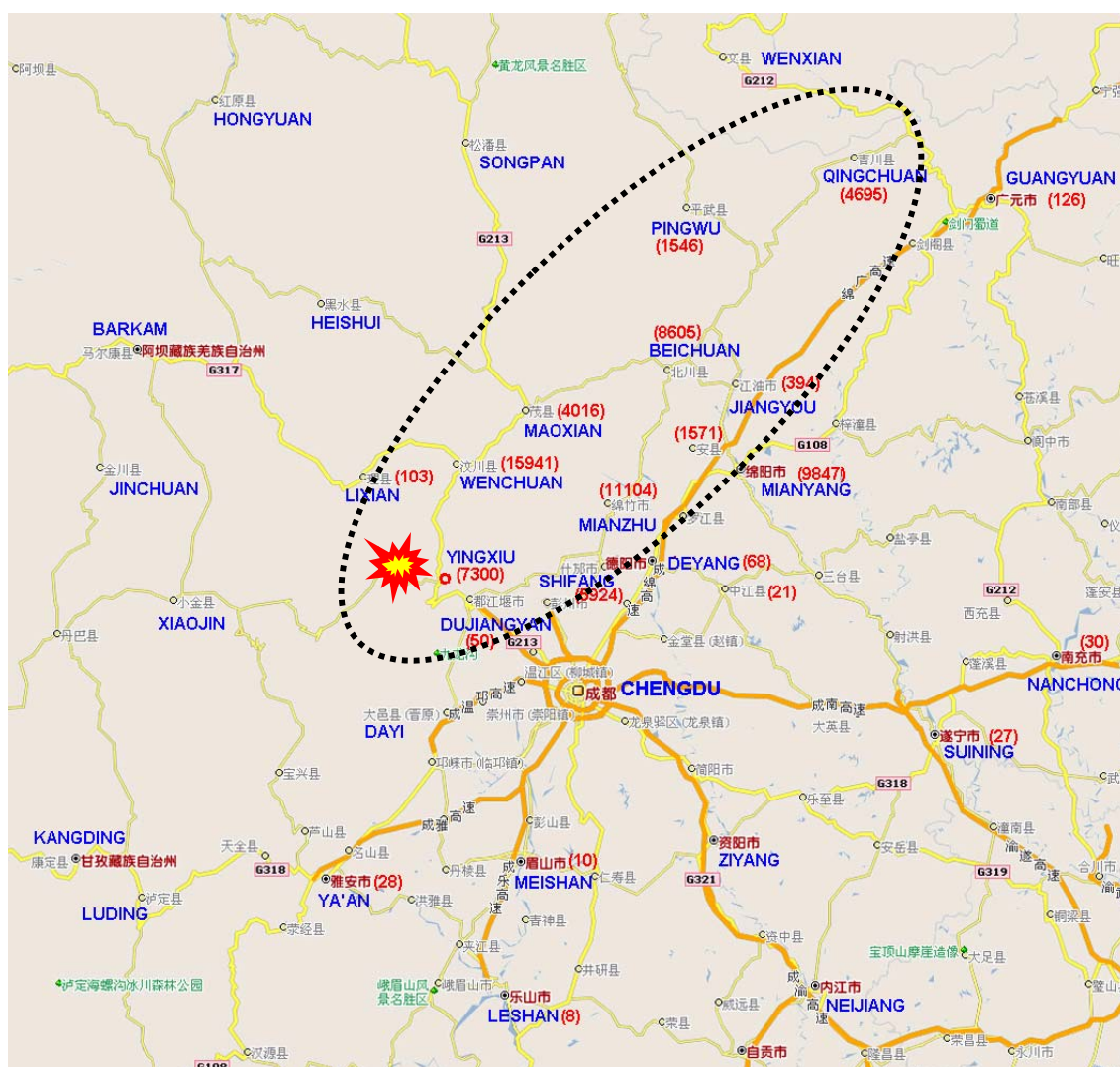


Figure 7.1 Earthquake affected cities and counties and number of casualties at each locality (base map from Google)

8 DAMAGE TO STRUCTURES

The authors had the chance to inspect damaged areas as shown in Figure 8.1. The investigation routes included major damage to civil engineering structures associated with ground motions and faulting. The results of the investigations together with the technical information available on several web-sites and deduced from pictorial images from web-sites by the authors are presented in this section.

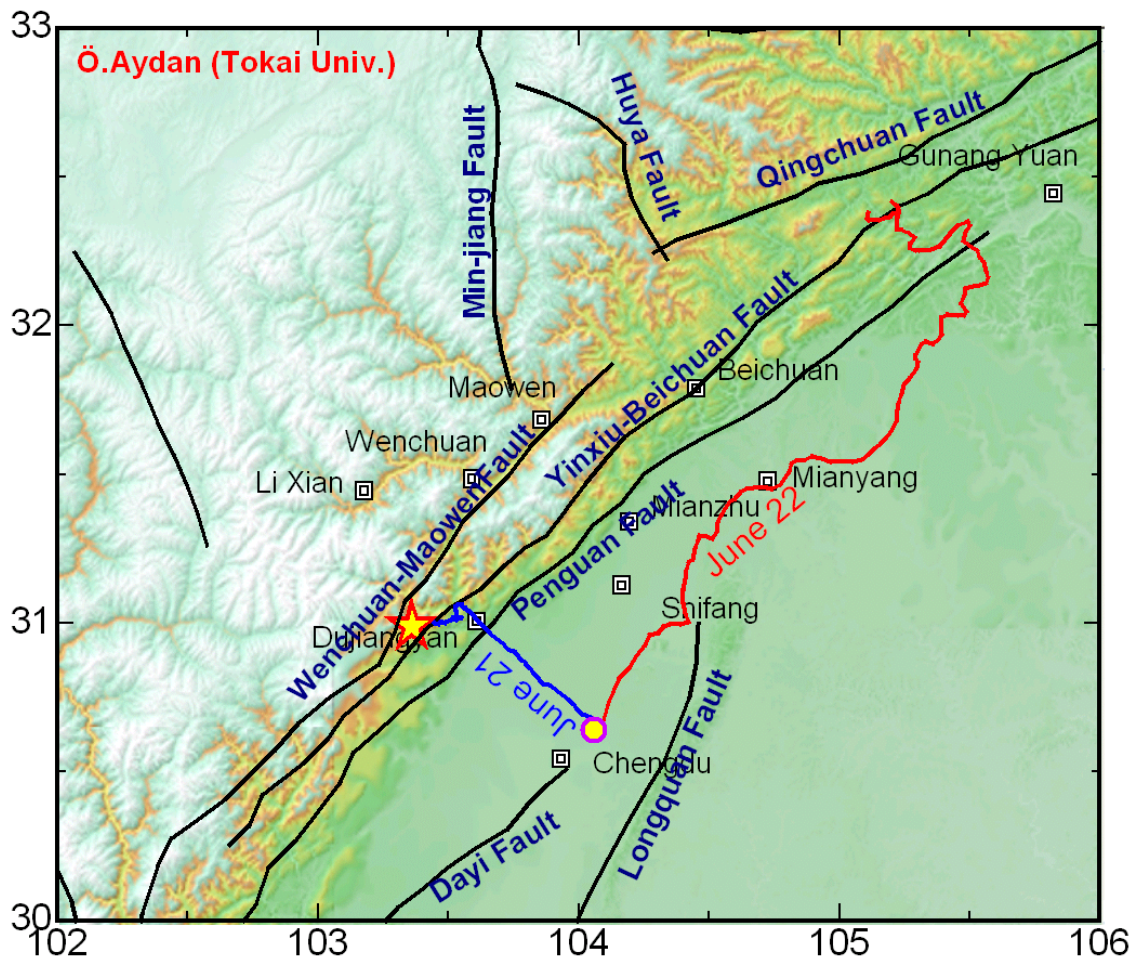


Figure 8.1. Investigation routes

8.1 Damage to Bridges

There are four bridge types in the epicentral area. Old bridges are stone arch masonry bridges. The second bridge type includes simply supported or arch cast-in reinforced concrete bridges. The third type bridges or high viaducts are with simply supported pre-cast reinforced concrete bridges. The fourth type are suspension bridges. Although

old stone masonry arch bridges generally performs well during earthquakes, they may collapse when there are permanent movements at abutments, piers or the both. Several examples of such collapses were observed in the earthquake epicentral area as shown in Figure 8.2.



(a) Hongbai county



(b) Chenjiaba

Figure 8.2. Views of collapsed stone masonry arch bridges (from Xinhuanet)

The second bridge type includes simply supported or arch cast-in reinforced concrete bridges. The simply supported cast-in place bridges performed very well during the earthquake. Except the settlement of embankment at abutments, the damage to such bridges were almost none or slight. However, some of these bridges become obstructed by rock slope failures at several locations and (Figure 8.3). Furthermore such bridges collapsed due to permanent movement of the abutment due to thrust faulting.



(a) Damage by rock slope failure



(b) collapse due to faulting

Figure 8.3. Damaged or collapsed bridges by rock slope failure or faulting (from Xinhuanet)

Reinforced arch bridges with short or long span are quite common in the epicentral area. These bridges generally performed well during the earthquake (Figure 8.4). However, there were some damage to the arch section of these bridges. The cracks run parallel to the perpendicular to the longitudinal axis of the bridge are thought to be due to movements of the abutments. The bridge is about 230km away from the epicenter and it is 6km away from the earthquake fault. In the vicinity of this small bridge, the stone masonry wall of a house was toppled and the inferred ground motion is expected to be more than 0.2g. It is expected that cracks observed should not be of great concern to its structural function.



Figure 8.4. Non damaged arch bridge (Qingchuan province)



Figure 8.5. Slightly damaged reinforced concrete arch bridge (32.43049N,105.23746E)

The heaviest damage occurred at the four span reinforced arch Hsiaoyudong bridge in Longmenshan town (Lin, 2008), from which the Longmenshan fault zone was named. The arch sections of the bridge were sheared as shown in Figure 8.6. Besides high ground motions in the vicinity of the bridge, the shearing of arched section in the longitudinal axis of the bridge implies permanent ground movements, which may result from thrust faulting and ground liquefaction beneath the riverbed.



Figure 8.6. Collapsed Hsiaoyudong bridge in Longmenshan town (pictures and figure from NRCEE, 2008)

One section of the highway named as Baihwa Bridge between Wenchuan and Dujiangyan, is a 500m long viaduct with a 30m height (Figure 8.7). The three-span convex part of the bridge collapsed during the earthquake. The girders were fallen towards the slope side while the columns were broken and fallen towards the river side. Although the authors did not visit this side yet, the impressions such that the permanent ground movements can be the key-factor besides the close proximity of the Baihwa bridge to the epicentral area.



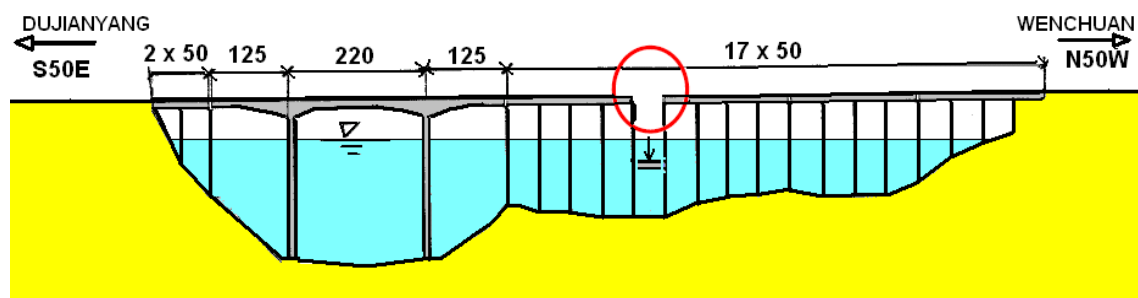
(a) Aerial view



(b) views of the collapsed sections (note the ground ruptures in foreground)

Figure 8.7. Views of the collapsed section of the Baihwa bridge (from Xinhuanet)

Miaoziping (Miaotzuping) bridge passes over Zipingpu dam reservoir. The bridge is 1436m long with a height of 100m (Figure 8.9). The main bridge is long span box girder bridge with 19 approaches with T-girders. The construction of the bridge was completed at the time of the earthquake. However, it was not open to traffic yet. The earthquake caused the shifting of bridge girders in longitudinally and laterally. One of the T-type girder approaches collapsed. The surveying indicated that the distance between piers was increased by more than 50cm and there were all-around fractures, spalling and bending cracks in the pier just above its foundation. While there were stoppers for lateral movements, there were no stopper longitudinally. Furthermore, the sliders (pedestals) were 40cm by 40cm.



Fallen section



Centerline offset



SE Side



NW Side

Figure 8.9. Sketch and views of the fallen section of the Miaoziping Bridge

Another section (N31.04392,103.52891, 15.4km away from the epicenter) of Wenchuan-Dujianyang expressway nearby the Miaoziping bridge was also damaged by the permanent movement of foundation ground resulting from earthquake induced slope movements (Figure 8.10). The foundation ground consist of debris material consisting of sandstone and shale. In the west abutment, the debris material is a thick deposit. Furthermore, there were also toppling and planar sliding of steeply inclined intercalated sandstone and shale depending upon the orientation of slope.



Figure 8.10. Damage to viaducts due to permanent displacement of foundation ground

The girder of the north approach of the Shoujiang bridge, which is about 9.8km away from the earthquake epicenter, was partially shifted and rotated (Figure 8.11). The south of the side of girder was offset from its pedestal and supported by a temporary scaffold. The site inspection of cracks of piers indicated that the foundation ground has moved towards south. In other words it moved towards the river. As a result of that movement, the bending cracks appeared on the southern side of two piers on the northern abutment. Nevertheless, No cracks were observed at the rest of other piers.

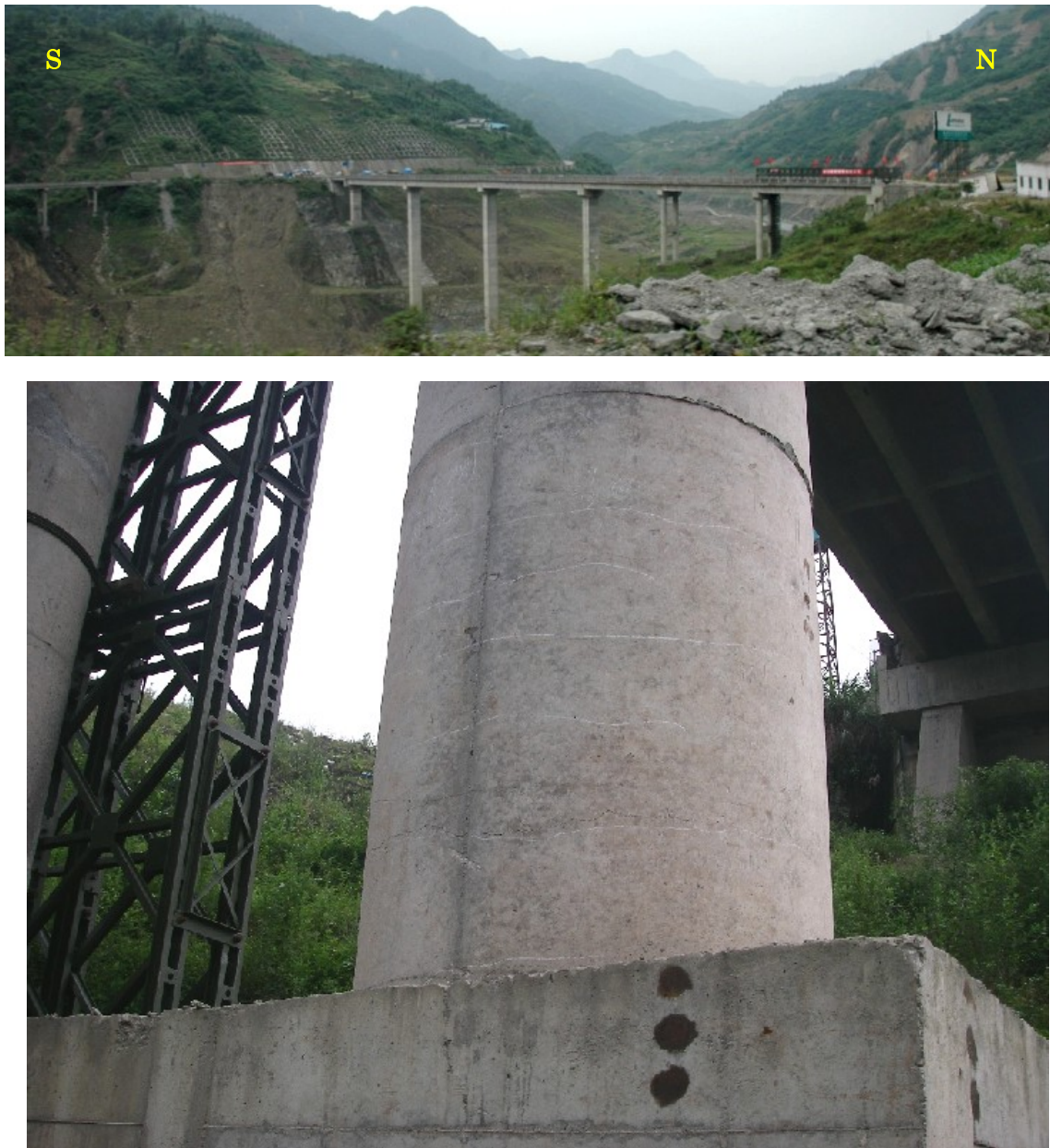


Figure 8.11. A view of damaged Shoujiang Bridge

The forth bridge type is suspension bridges. There is a cable stayed bridge near Jiangyou on the expressway between Chengdu and Guanyuan. There was no visible damage to this bridge (Figure 8.12). However, There were some damage to suspension bridges for pedestrians due to the movement of anchorage blocks (Figure 8.13).



Figure 8.12. View of the cable-stayed bridge near Jiangyou



Figure 8.13. Damage to some pedestrian suspension bridges (from Xinhuanet)

8.2 Damage to Roadways and Railways

Damage to roadways was mainly caused by slope and embankment failures and rock falls (Figure 8.14, see Figure 7.1 for locations). In some places such as Yingxiu, Beichuan and Qingchuan, the damage to roadways and railways was caused by faulting (see Figure 5.3). The highways G213 and G317 were obstructed at numerous locations. The damage to the pavements of roadways by ground shaking could not be observed. The damage to Chengdu-Guangyuan expressway was observed in the section between Deyang and Mianzhu junctions due to the embankment failure. Nevertheless, the damage was limited and the expressway was open to traffic soon after the earthquake. One of the distinct characteristics of this earthquake is too many crushing of vehicles by the rockfalls, which probably deserves further detailed studies as a lesson of this earthquake.



Figure 8.14. The obstruction of roadways due to rock slope failures



Figure 8.15. Rockfall induced damage and vehicles crushed by rockfalls (partly from Xinhuanet)



Figure 8.16. Views of damage to highways due to embankment failures (partly from Xinhuanet)

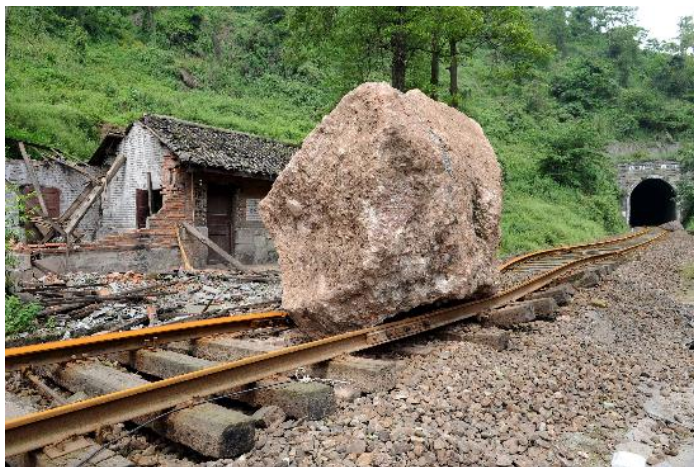


Figure 8.16. Views of damage to railways ,(from Xinhuanet)

8.3 Damage to Tunnels

There are many roadway and railway tunnels. Some of them are under construction. It is well known that the underground structures are earthquake-resistant compared to surface structures when ground shaking is concerned. The damage to tunnels are generally limited to portals, which are mainly caused by slope failures and rockfalls. Several examples of portal damage are shown in Figure 8.17. Similar damage to portals of railway tunnels were also observed. Nevertheless, such damage are light in scale and did not cause any major structural stability problems so far.



Figure 8.17. Damage to tunnel portals

The authors had the chance to visit five tunnels, three of which were under construction and suffered heavy damage during the earthquake. The tunnel nearby Zipingpu dam (N31.04888,E103.56463) is a two lane tunnel with a length of about 1000m. The lining was damaged at several locations perpendicular to its longitudinal axis, which is aligned NW-SE direction. This tunnel was already repaired at the time of the investigation (June 21, 2008) (Figure 8.18). The tunnel is about 18.5km away from the earthquake epicenter and it is very close to the Yingxiu-Beichuan fault. The tunnel floor was stepped at the damaged zones implying the NW side is moved upward. Since this earthquake is of great scale and its relative slip was presumed to be about 7m, it is very natural to expect a diluted deformation zone as the fault approaches the ground surface due to the reduction of vertical stress. The damaged section of the tunnel rebolted and shotcreted.

Longxi tunnel is a part of Wenchuan-Dujiangang expressway. Double laned two tunnels are excavated with a 3D wide pillar. The maximum overburden is about 480m and the maximum in-situ stress is about 26 MPa. The fault named as F8 is 900m from the SE portal and its strike is perpendicular to the longitudinal axis of the tunnel. The engineers informed the authors that they had difficulty of maintaining the stability and controlling the deformation of the tunnel during excavation.



Figure 8.18. Views of repaired damaged section of the tunnel nearby the Zipingpu dam

The tunnel was excavated using the rockbolts and shotcrete as an initial support and then the unreinforced concrete lining was constructed. The concrete lining was ruptured and the crown concrete was fallen down (Figure 8.19). However, the overall rupture

trace dips NW. The floor of the tunnel is also ruptured and uplifted by buckling. The tunnel collapsed at the location where the overburden is about 70m. The collapse may have created a sinkhole at the ground surface, which should be checked. The similar type of the collapse occurred at the Elmalik section of Bolu Tunnel during the 1999 Duzce-Bolu earthquake (Aydan et al. 2000). As the ground conditions at both tunnels remarkably similar to each other. The engineers still did not checked the zone beyond the collapsed section of the tunnel. The fundamental causes of the damage to this tunnel is probably the permanent ground deformations along the fault zones as well as high ground shaking.



Figure 8.19. Views of earthquake damage at Longxi (Longqi) Tunnel

Jiujiaya Tunnel is a 2282m long double lane tunnel and the coordinate of its south portal is N32.41288 and E105.12046. The tunnel is 226.6km away from the earthquake epicenter and it is about 3-5km away from the earthquake fault of Wenchuan earthquake. The tunnel face was 983m from the south portal at the time of the earthquake (Figure 8.21). The concrete lining follows the tunnel face at a distance of approximately 30m. The tunnel suffers from metan gas problem due to coal seams below the tunnel. The rock consists of phyllite with intercalations of dolomite. The bedding planes has the orientation of NW50/64, which is roughly similar to that of the Longmenshan fault zone. The geological investigation indicated that the tunnel pass through several fracture zones. The engineers informed the authors that 30 workers were working at the tunnel face and one worker was killed by the flying pieces of rockbolts, shotcrete and bearing plates caused by intense deformation of the tunnel face during the earthquake. The concrete lining was ruptured and fallen down at several section (Figure 8.22). However, the effect of the lining rupturing was quite large and intense in the vicinity of the tunnel face. The rupturing of the concrete lining generally occurred at the crown sections although there was rupturing along the shoulders of the tunnel. Furthermore, the invert was uplifted ue to buckling at the middle sections. Sometimes, the whole invert was pushed upward. The authors noticed that the tunnel heading was offset in a dextral sense with an upward with respect to the rest of the tunnel. The lateral and vertical offset displacements are approximately 100mm. This sense of deformation is very similar to that of the Longmenshan fault zone, which probably cuts through the tunnel with an acute angle of 50-60°. Besides the high ground shaking, the permanent ground deformations definetly played an important role on the damage observed in Jiujiaya Tunnel.



(a) South portal

(b) Tunnel face

Figure 8.21. Views of the south portal and the heading of Jiujiaya Tunnel



Figure 8.22. Views of damage at Jiujiaya Tunnel

8.4 Damage to Pylons and Poles

The preliminary site investigations and additional data and information other sources clearly indicated that the damage to pylons and poles were either caused by the collapse of buildings, slope failures or faulting. The effect of ground shaking on the damage to pylons and electricity poles seems to be small (Figures 8.22 and 8.23. Particularly the selection of foundation ground for high pylons and their structural design and construction should have been very carefully implemented.



(a) Damaged or broken utility poles



(b) Non-damaged utility poles

Figure 8.22. Views of damaged or non-damaged reinforced concrete utility poles



Figure 8.23. Views of damaged and non-damaged pylons

8.5 Dams and Power Houses

There are around 400 dams in the area of the earthquake, with four dams being classed as major dams with heights more than 100m (Figure 8.24). The nearest dam to the epicenter is Zipingpu dam built in 2006 with a height of 158m and it is concrete faced rock fill dam. The Zipingku Dam is about 9 kilometers upstream from the small city of Dujiangyan. The surveying indicated that the abutments of the dam moved inward and the maximum displacement was 101.6mm. The settlement of the crest of the dam was 734.6mm with a 179.9mm displacement towards the downstream side. (Figure 8.25). The seepage of the dam changed from 10.38l/s to 15.07 l/s. The Zipingpu dam was designed for the base acceleration of 0.26g but the acceleration at the crest during the earthquake was greater than 2g. The gates and power generating units were damaged by the earthquake.

The Shapai dam is 32m high and it is an arch RCC (roller compacted concrete) dam. it is located only 12 km from the epicentre. It has been reported that there is no immediate danger to this dam. Although this RCC dam was designed for a base acceleration of 0.138g, it could have been was subjected to much higher acceleration. Nevertheless, such records are not available for this dam.

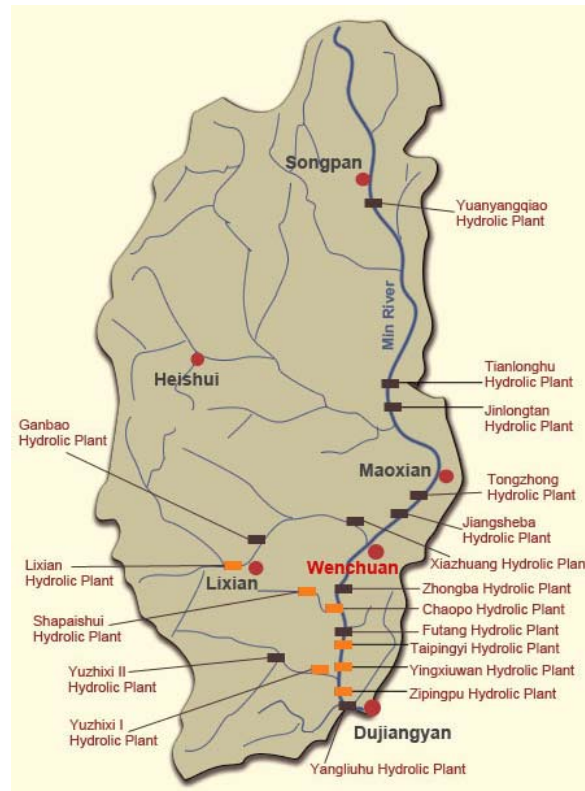


Figure 8.24 Dams in the epicentral area

Bikou is a 101.8m high clay core dam built in 1976 with a capacity of 0.5Bm³ and Bailonghu dam, is a 137m high gravity dam built in 1997 with a capacity of 2.52 Bm³. Both dams are located near the provincial boundary between Sichuan and Gansu provinces on Jialing river. Bikou dam is the largest earthfill dam and the crest was settled more than 240mm and moved 250mm horizontally towards the downstream side. Both dam provides water to Baozhusi hydroelectric power plant. The both experienced the quake with an intensity of 7, but both were designed for magnitude 7 according to Chen, and no damage has been reported. The landslide had blocked the flows of the White River, creating an artificial lake in its upstream, near the Kuzhuba hydrolic dam. If the water pressure built up and threatened to burst the dam



Figure 8.25: Views of Zipingpu dam

8.6 Industrial Facilities

There are many industrial plants in Chengdu and its close vicinity. Chengdu is China's fifth largest city and has a high-tech industrial development zone where companies such as IBM, Symantec, Microsoft, Intel, Fujitsu, Corning, Ericsson, Semiconductor Manufacturing International Corp. (SMIC), Nokia and Monolithic Power Systems, among others, have established operations. Except, the effect of ground shaking, there was almost no damage report for industrial facilities in Chengdu. Furthermore, Sichuan province is known for its petroleum and natural gas reserves. The preliminary reports indicate that there was also no structural damage to these facilities.

The heavy damage to industrial facilities were observed in Hongbai and Hanwang towns near Shifang, where ground accelerations up to 632 gals were recorded. These towns are 75km away from the epicenter. However, they are in the close proximity of the earthquake fault (within 15-20km). The reports indicated that two chemical plants were heavily damaged in Hongbai town (Figure 8.26 and 8.27). These plants released more than 80 tons of liquid ammonia. There are also some damage to industrial facilities in Yingxiu and Wenchuan (8.28).



Figure 8.26. Some examples of damage to industrial plants in Hongbai



Figure 8.27. Some examples of damage to industrial plant in Hanwang



Figure 8.30. Views of damage to industrial facilities at Yingxiu town

9 SLOPE FAILURES AND QUAKE LAKES

9.1 Slope failures

One of the most distinct characteristics of 2008 Wenchuan earthquake is the widespread slope failures all over the epicentral area. The term of slope failure is preferred herein and the landslide is considered to be a special form of slope failures involving slippage on a curved or planar failure surface. Slope failures, which are fundamentally similar to those observed during 2005 Kashmir earthquake, may be classified into three categories as follows (Figure 9.1):

- a) Soil slope failures
- b) Surficial slides of weathered rock slopes
- c) Rock slope failures
 - Curved or combined sliding and shearing failure
 - Planar Sliding (active and passive)
 - Wedge sliding failure
 - Flexural or Block Toppling (active and passive)

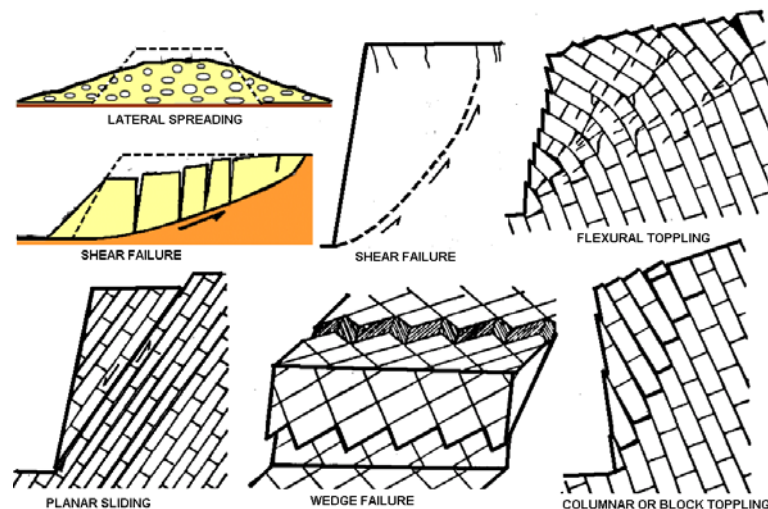
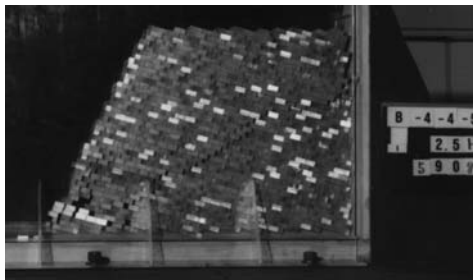


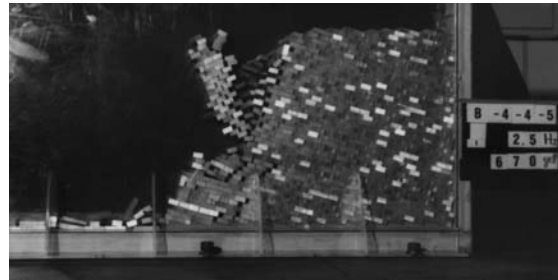
Figure 9.1. An illustration of slope failures (from Aydan and Hamada, 2006)

In addition to the failures shown in Figure 9.1, some passive forms of sliding and toppling failures were observed. Figure 9.2 shows some pictures of model tests on jointed rock mass with a thoroughgoing discontinuity set carried out during 1984-1986 at Nagoya University by the first author and his colleagues (i.e. Shimizu et al. 1988, Aydan et al. 1989, 2006a, 2006b). To initiate passive modes of sliding and toppling failures, it should be noted that very high ground accelerations are necessary. The

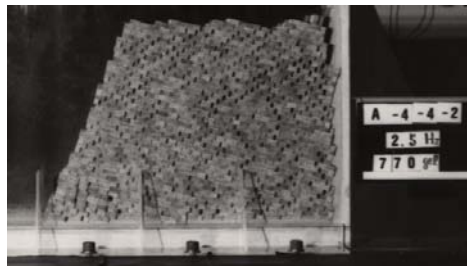
passive mode is defined when the vertical component of the movement of the unstable body of the slope is upward. The relative displacement of the block on the sliding plane at the toe of the slope should be greater than its half-length for the collapse of the slope in passive sliding mode. When such relative movements take place, the initial sliding movement changes its character to the rotational mode. As a result, the unstable part of the slope rolls down the slope. As for the passive toppling mode, the blocks in the upper part of the slope rotates and rolls down. So many rock falls observed during this earthquake are related to these two phenomena.



$a_{max} = 590$ gals



$a_{max} = 670$ gals

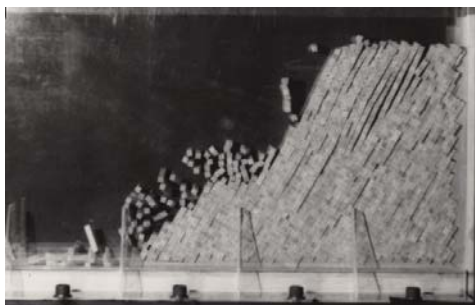


$a_{max} = 770$ gals

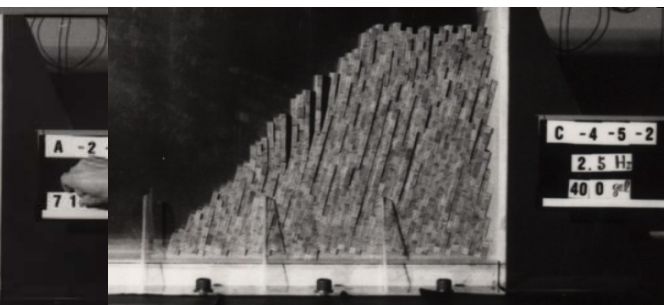


$a_{max} = 780$ gals

(a) Passive sliding and subsequent rotation of unstable part of the slope



$a_{max} = 710$ gals



$a_{max} = 400$ gals

(b) Passive toppling of blocks of unstable part of the slope

Figure 9.2. Several views of model tests on jointed rock slopes with a thoroughgoing discontinuity set during 1984-1986 at Kawamoto Laboratory of Nagoya University (Shimizu et al., 1998; Aydan et al. 1989, 2006a, 2006b)

9.1.1 Weathered Rock Slope Failures

Rock units in the epicentral area are phyllite or slate, sandstone, mudstone, shale and limestone. Particularly reddish mudstone and brackish shale are very prone to weathering. Furthermore, the rocks at higher elevations are also subjected to thawing and freezing as well as other atmospheric conditions. Most of these rock units contain joints, bedding or schistosity planes as well as fracture zones due to intense tectonism associated with Longmenshan fault zone. In addition, the limestone is very prone to solution by percolating ground water along fractures and they contain many solution cavities. Figure 9.3 shows several surficial slope failures in limestone unit in the vicinity of the Weizhou and the Zipingpu dam site. The surficial slope failures in limestone unit was spectacular and continued for several kilometers as they are clearly noticed in satellite images.



Figure 9.3. Spectacular surficial rock slope failures

9.1.2 Rock Slope Failures and Rockfalls

As said above, rock units are phyllite or slate, sandstone, mudstone, shale and limestone. Geologically, granitic unit exist in the epicentral area. However, the authors did not have chance to see such sites. Except granite, all rock unit has at least one throughgoing discontinuity set, namely, bedding plane or schistosity plane. Since rock units had been folded, they also include joint sets and fracture planes as a result of tectonic movements. Furthermore, the measurements on faults in limestone outcrops in the vicinity of Miaoziping bridge indicated three dominant faults, which divide the limestone unit into large blocks. Granite generally has at least three discontinuity sets. In regard with rock slope failures classified in Figures 9.1 and 9.2, the rock slope failures are mainly planar sliding, flexural or block toppling failure (Figure 9.4). In addition, passive sliding and toppling failures were observed in intercalated sandstone and shale units.

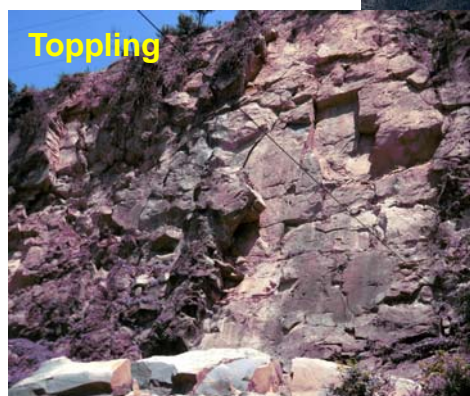


Figure 9.4. Some examples of rock slope failures and rock falls

Active planar sliding failures were probably much larger in scale as compared with other slope failures. Several large scale slope failures will be presented and discussed in next sub-section. Rockfalls in the epicentral area are generally result of the toppling of rock blocks due to excitation of the earthquake. Numerous rockfalls were observed for a great length of roadways. Rockfalls were common in sandstone and limestone slopes, which caused a huge number of vehicle crushing events resulting in heavy casualties.

9.1.3 Large Scale Slope Failures – Landslides

The satellite images and in-situ investigations indicated that there were very large scale slope failures along the earthquake fault zone. These large scale events took place in Xuankou(Yingxiu) (SW tip), Beichuan (central part, three large scale slope failures including the Tangjiashan landslide) and Donhekou village (NE tip). All these large scale slope failures were visited by the authors. The characteristics of these large scale slope failures are briefly explained in this subsection.



Figure 9.5. A view of the Yingxiu landslide

(a) Xuankou(Yingxiu) Landslide

The Yingxiu landslide (Figure 9.5) involved mainly limestone, which dips to the valley side with an inclination of $20-25^{\circ}$. Furthermore, there is a fault dipping parallel to the failure surface within the rock mass. The angles of the lower and upper parts of the failed slope are 60° and 30° , respectively. In addition to this new landslide, one can

easily notice the existence of a paleo-landslide in the fore-ground. The failure plane of this slope failure or landslide is bi-planar and it involved the fault and bedding plane. The fault plane probably assisted the separation of the failed body from the rest of the mountain. The in-situ tilting tests on the limestone joint surfaces yielded the friction angle as $38-42^{\circ}$. If the resistance is purely frictional the expected lateral horizontal seismic coefficient should be greater than $0.36g$. Since Yingxiu town was heavily damaged by this earthquake, it is more likely that such a high ground acceleration did act on this slope.

(b) Beichuan Landslides

There are several large landslides in Beichuan town and its close vicinity including the Tangjashan landslide (Figure 9.6). UNOSAT (2008) recently released a topographic map of the area (unfortunately such topographic maps are generally inaccessible in China) and a part of this topographic map is shown in Figure 9.7. In association with the sliding motion of the earthquake fault, NW or SE facing slopes failed during this earthquake. There were two large scale slope failures (landslides) in Beichuan county, which destroyed numerous buildings and facilities. The NW facing landslide (Jingjiashan) involved mainly limestone while the SE facing landslide (Wangjiaya) involved phyllite (it is mudstone and sandstone according to some) rock unit, which is folded with the antcline axis plunging NE (Figure 9.8). Limestone layers dips towards the valley side with an inclination of about 30° . Furthermore, there are several faults dipping parallel to the failure surface within the rock mass. The angles of the lower and upper parts of the failed slope are 60° and $30-35^{\circ}$, respectively. The existence of several faults dipping parallel to the slope with an inclination of about $60-65^{\circ}$ creates a stepped failure surface. If the resistance is assumed to be purely frictional the expected lateral horizontal seismic coefficient should be greater than $0.18g$.

The SE facing slope (Wangjiaya landslide) may involve a slippage along the steeply dipping discontinuity plane (fault plane ?) and shearing through the folded rock mass. In other words, it may be classified as a combined sliding and shearing failure (Aydan et al. 1994). The angles of the lower and upper parts of the failed slope are $40-45^{\circ}$ and $30-35^{\circ}$, respectively. The layers dip at angle of 40° towards the valley and shearing plane is inclined at an angle of 20° . Since material properties and conditions of rock mass are not well-known for this site yet, no estimation on possible ground acceleration has been done. Nevertheless, it is more likely that such a high ground acceleration did act on this slope since Beichuan town was heavily damaged by this earthquake.

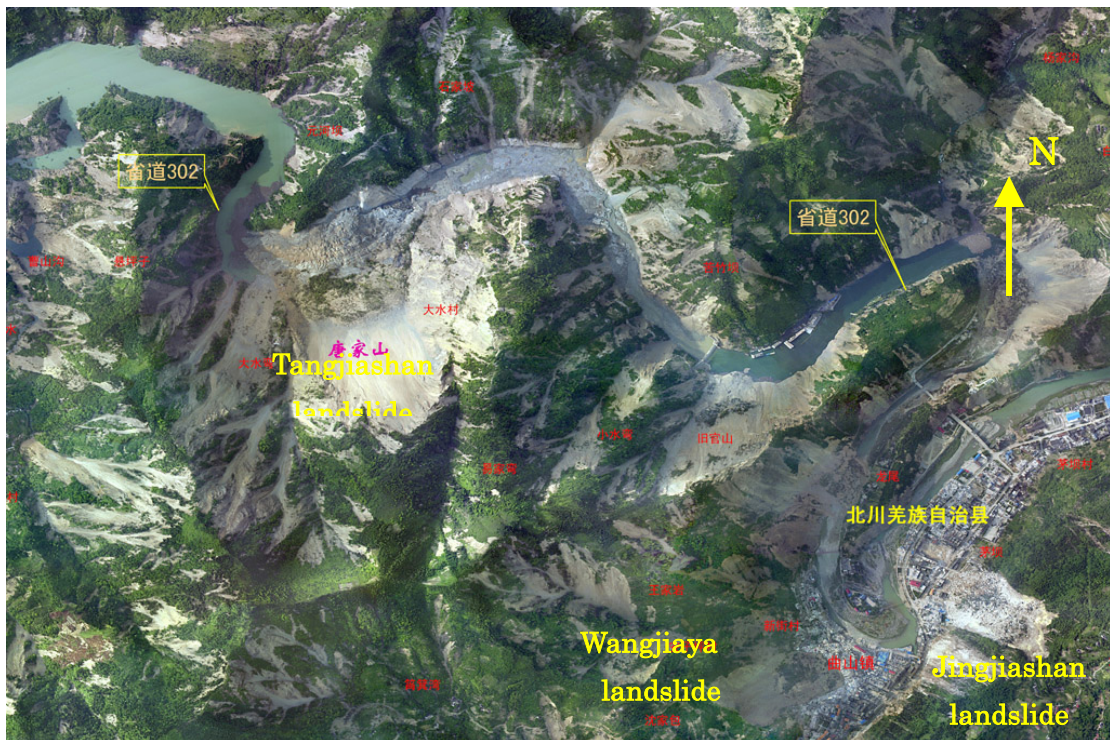


Figure 9.6. A satellite view of Beichuan and its close vicinity (modified from CGSI)

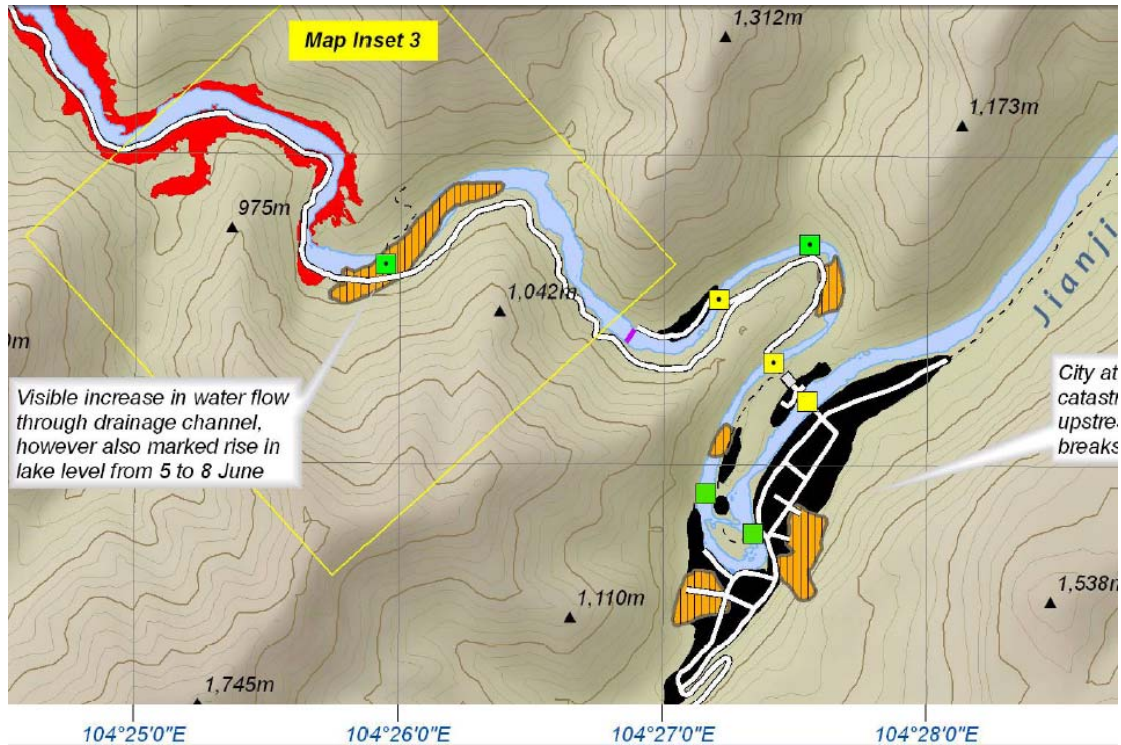


Figure 9.7. A topographic map of landslides in Beichuan and close vicinity (modified from UNOSAT, 2008)



Figure 9.8. Views of landslides in Beichuan

Tangjiashan landslide, which obstructed Jian River, is located about 2km NW of Beichuan (Qushan) town (Figure 9.9). The landslide faces NW. The rock units involved in this landslide is limestone (top part), and intercalated sandstone and shale (lower part). Rock layers dip towards the valley at an inclination of $40-50^{\circ}$, Although the upper part of the mountain has a slope angle of $40-45^{\circ}$, the lower part is more steeply inclined up to 70° due to the toe erosion by Jian River. The earthquake induced almost a planar sliding of 600m wide and 450m long body of rock mass. This landslide blocked Jian River for a length of 800m and created a landslide dam with a maximum height of 124m.

This landslide occurred at Donghekou village of Hongguang Township, Qingchuan County and it is located at the NE tip of the earthquake fault. The upper part of the mountain covered by limestone, below which phyllite exist. This phyllite formation is considerably thick and it is inclined at an angle of $30-45^{\circ}$ to NE and it is slightly discordant with upper limestone formation. A paleo landslide exist to the east of the new landslide source area. The in-situ tilting tests on the phyllite schistosity (bedding) plane surfaces yielded the friction angle as $22-24^{\circ}$, which is considerably small. In other words, slopes facing NE can not be stable even under static conditions if the resistance is only frictional. The initial movement of the unstable part of the mountain should have

been in NE direction and then its direction of motion rotated towards SW (Figure 9.10). Further investigations and laboratory tests on samples from this site should provide essential parameters for investigating the conditions for the failure of the slope at this site.



Figure 9.9. A view of Tangjiashan landslide (arranged from the image by Xinhuanet)



Figure 9.10. A view of Donghekou landslide in Qingchuan County

9.2 Mitigation Measures

The mitigation measures against huge slope failures and rockfalls must be based upon the knowledge and know-how of modern rock slope engineering. Most of roadways were obstructed by the slope failures in the epicentral area. The debris of failed slopes should be cleared from top to bottom. Following the clearance of the failed part, an utmost care should be taken against the stabilization or clearance of the loose part. If possible, rockbolts, rockanchors with wire meshes and shotcrete could be utilized (Figure 9.11). However, it should be noted the shotcrete has no structural support effect except preventing the small scale falls and erosion. Furthermore, the slope failures were analyzed together with some computational results from previous studies by the first author. The results are shown in Figure 9.12 and this figure was prepared as a guideline for local engineers how to select the slope-cutting angle in actual restoration of the failed slopes.

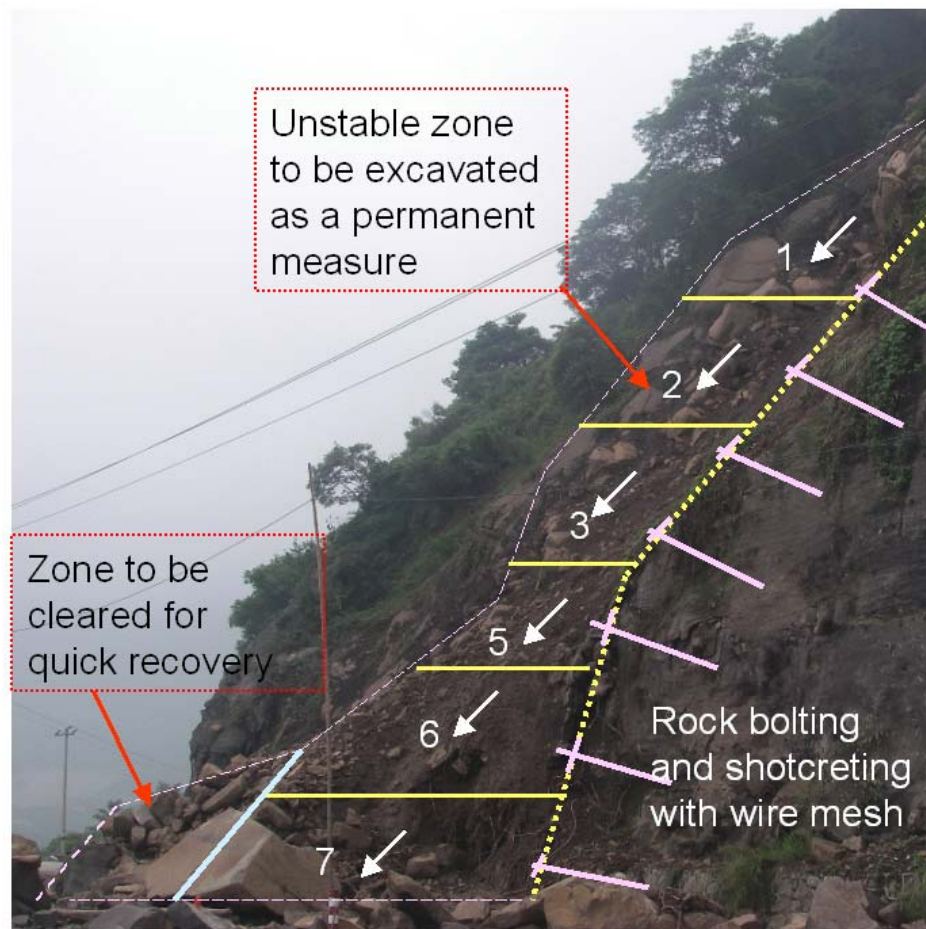


Figure 9.11. Proposed quick recovery and permanent measures for the restoration of failed slopes (Hamada and Aydan, 2008)

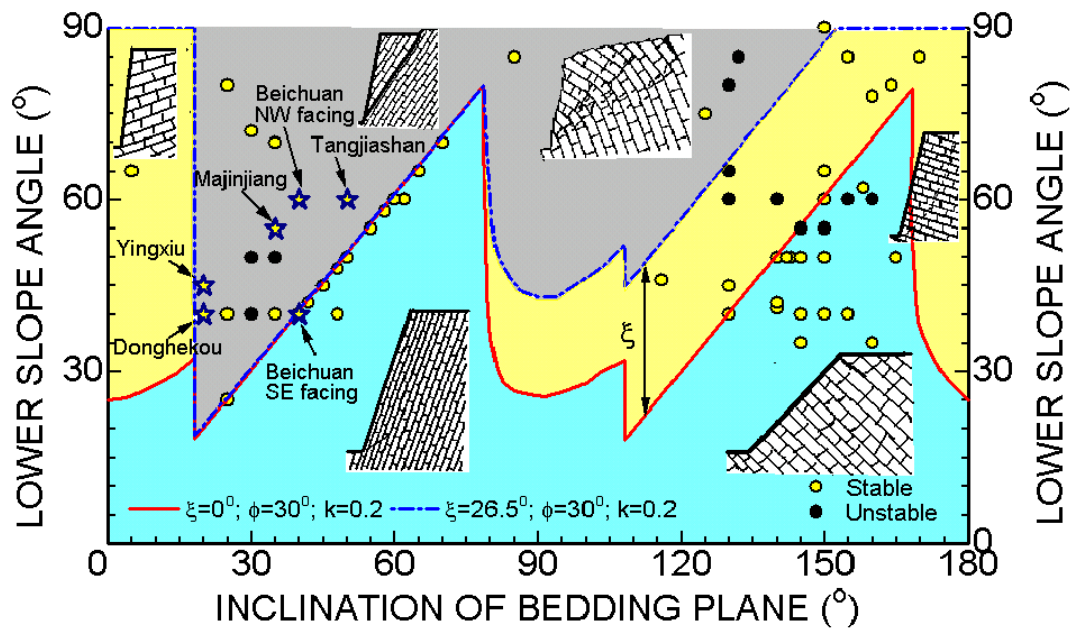


Figure 9.12. Proposed guideline for slope-cutting angle in relation to the bedding plane angle for the restoration of the failed slopes (ξ : intermittency angle; k : horizontal seismic coefficient; ϕ : friction angle).

9.3 Quake Lakes (Landslide Dams)

The 2008 Wenchuan earthquake caused the formation of 34 quake lakes. Figure 9.13 shows the location of major quake-lakes and Figure 9.14 shows pictures of some of quake-lakes before breaching.



Figure 9.13. Locations of major quake-lakes



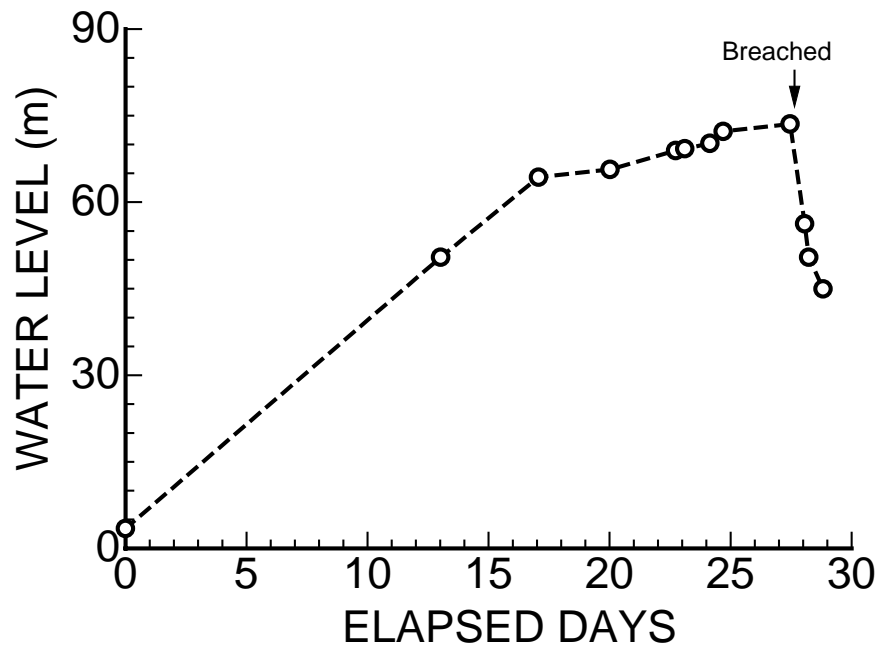
Figure 9.14. Views of some of quake lakes before breaching (partly from Xinhuanet)

Among 34 quake-lakes, three quake-lakes formed in Anxian, Qingchuan and Beichuan counties, were of great scale and were caused by mainly the planar sliding failure of mountains. Among all, the biggest quake-lake was the Tangjiashan "quake lake", which was formed by the collapse of a section of Tangjiashan Mountain. Tangjiashan quake-lake was formed 2 km from Beichuan and at its peak was 803m long by 612m wide and 70-124m high. The estimated volume of water of the Tangjiashan quakelake was 250M m^3 . Initially several spillways were constructed. However, the drainage through constructed spillways was not successful and several leakages occurred. At the final stage, explosives were used to create channels. However, these measures were not sufficient and missiles were used to control the drainage and erosion of the flow path (Figure 9.15, pictures by Xinhuanet (2008)). This dangerous operation resulted in a successful drainage of the Tangjiashan quake-lake almost one-month elapsed after the

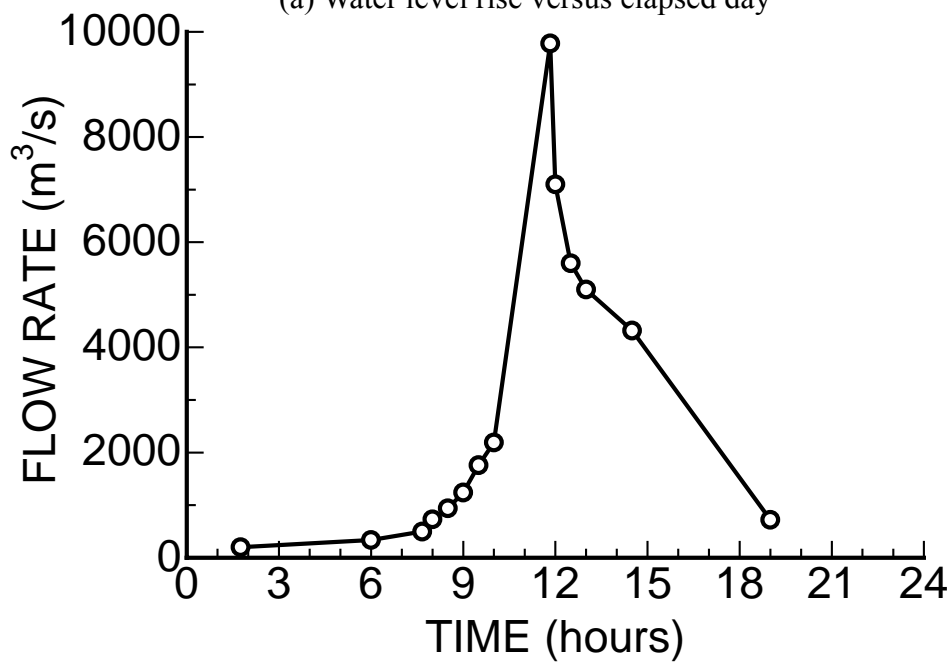
earthquake and a peak discharge of 980 m³/s was observed at 11:50 on June 10. Some 250,000 people downstream had already been evacuated during the drainage on June 10, 2008. Figure 9.16 shows the water level rise between May 12 and June 10 and drainage flow rate on June 10.



Figure 9.15. Views of several stages of Tangjiashan quake-lake (from Xinhuanet)



(a) Water level rise versus elapsed day



(b) Discharge rate in June 10 during which the landslide dam was breached

Figure 9.16. The water level rise between May 12 and June 10 and drainage flow rate on June 10 (data from China Water Resources)

In Anxian county, the second largest quake lake was caused by a landslide blocking Chaping River (Chapinghe) and it is named as Majingjiang. This quake-lake submerged Shuangdian village. Majingjiang (Chapinhe) quake-lake was estimated to be 40m deep and water was rising at a rate of 2.5m per day. The troops used construction machinery to create spillways of 2m wide to drain the quake-lake. This operation was successfully completed on June 6. However, the quake lake burst the remaining bank and drained through the constructed spillway (sluice). The operator of the machinery was lucky to save his life during the breaching of the remaining banks of the landslide dam. The huge landslide, which buried the village of Donghekou and two other small villages, blocked Qingzhu River in Qingchuan County. This landslide also resulted in two quake lakes. However, these quake lakes were successfully breached using construction machinery as well as blasting technique (Figure 9.17). The lower quake lake is not fully breached and one can still see the top of electricity utility poles.



Figure 9.17. Views of the drainage of Donghekou quake-lake

The 2008 Great Wenchuan earthquake in Sichuan Province of China caused the failure of natural slopes as well as cut-slopes besides the extensive damage to buildings, infrastructures and the loss of lives of more than 85000 people. The scale of slopes failures was tremendous and they indicated the vulnerability of natural slopes against failure during earthquakes, which are stable under non-seismic conditions. This topic probably deserves further studies and it implies the necessity of developing susceptibility maps of natural rock slopes against failure during earthquakes together with the consideration of discontinuous nature of rock mass. In addition, there were numerous rockfalls causing heavy casualties and damage in transportation system as well as buildings. Although it is a difficult topic to be dealt with, it is an urgent issue to be studied and addressed. If it is possible, rockbolts, rockanchors with wire meshes and shotcrete could be utilized to stabilize the disturbed slopes in the earthquake-affected area. Figure 9.12 may serve as a guideline for local engineers how to select the

slope-cutting angle in actual restoration of the failed slopes. The so-called quake-lakes have a high potential to cause secondary disasters following the earthquakes by breaching or slippage due to piping. When their scales are so large as in the case of Tangjiashan quake-lake, the successful drainage or sustaining their stability by the construction of spillways are not easy issues to be dealt with. Nevertheless, the quake-lakes caused by the 2008 Wenchuan earthquake were successfully drained through the utilization various techniques together with software measures such as evacuation people to higher ground in spite of several unsuccessful hardware attempts. The Wenchuan earthquake also showed that underground structures, especially tunnels, are vulnerable to sever damage when they are constructed in active fault zones. If the linings could not accommodate the deformation, there may be collapses of non-reinforced concrete linings. In such zones, the linings must be constructed as reinforced. As for existing non-reinforced tunnel linings in active fault zones, some counter-measures must be introduced to retrofit it with steel platens or fiber-reinforced polymers with rockbolts.

10 LIQUEFACTION AND LATERAL SPREADING

As expected from the magnitude of this earthquake, the liquefaction of sandy ground is very likely. However, the epicentral area along the rupture zone is mountainous and valleys are very narrow. The cities, towns and villages are located on relatively flat areas where rivers meander (Figure 10.1). The heavy structural damage in towns of Yingxiu and Beichuan were caused by permanent ground deformations due to faulting, slope failures (including so-called landslides) and lateral spreading resulting from strong ground shaking as well as ground liquefaction (Figure 10.2 to 10.4). The situation is quite similar to that observed in 2005 Kashmir earthquake (Aydan and Hamada, 2006, Aydan et al. 2008). Since the heavy structural damage was due to the combined action of various causes, it is very difficult to separate the ground liquefaction and its effect from other causes. However, the authors did observed some traces of liquefaction and lateral spreading from their investigations as well as available pictures on this earthquake (Figures 10.3 and 10.5). Except Yingxiu town, the authors did not have chance to visit the towns of Beichuan and Whenchuan. Nevertheless, one can easily distinguish the traces of liquefaction and associated geomorphological changes such as sandboils, lateral ground movements, settlement from available high resolution pictures and site investigations along the routes.

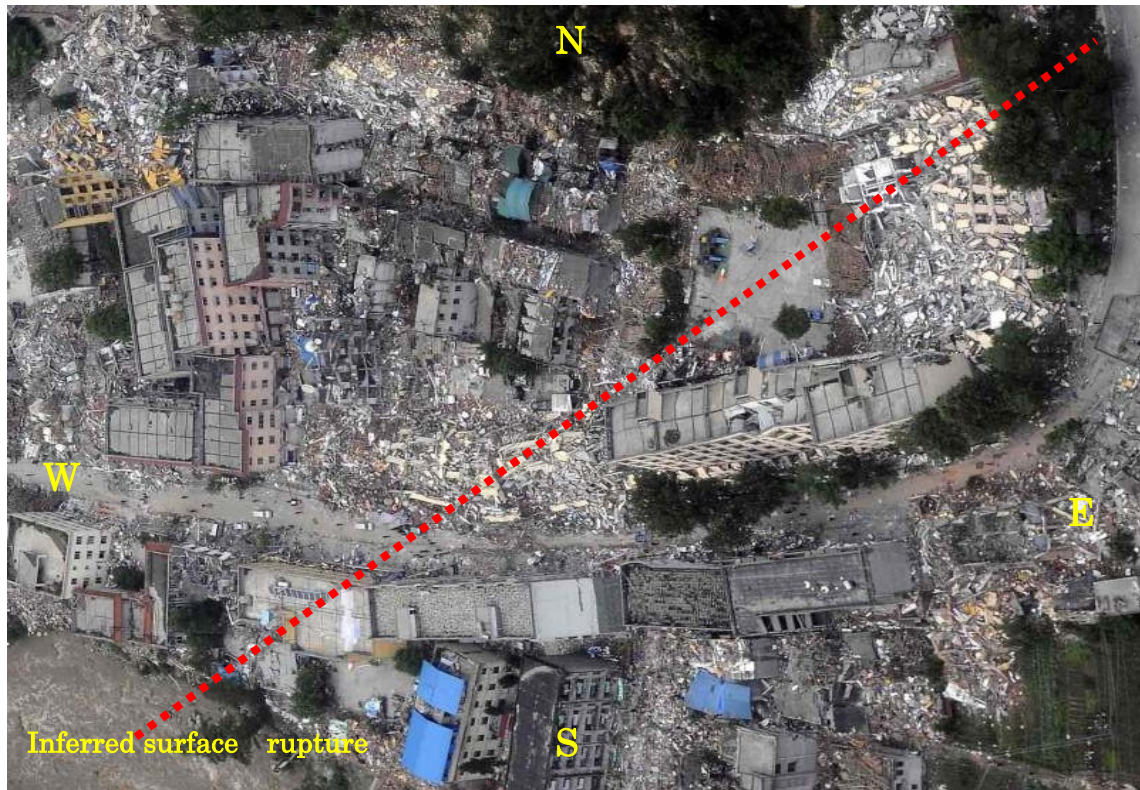


Figure 9.1. An aerial view of a heavily damage section of Yingxiu town

The sandy ground is observed along riverbanks. The traces of ground liquefactions could be observed in various locations along the inspected routes. Nevertheless, further geotechnical investigations of ground are desirable particularly in Yingxiu, Wenchuan and Beichuan in association with heavy structural damage.

Figure 9.6 compares the available Wenchuan earthquake data with those from other earthquakes regarding the relation between earthquake magnitude and liquefaction limit distance. The data of the Wenchuan earthquake is within the empirical bounds and data from past earthquakes.

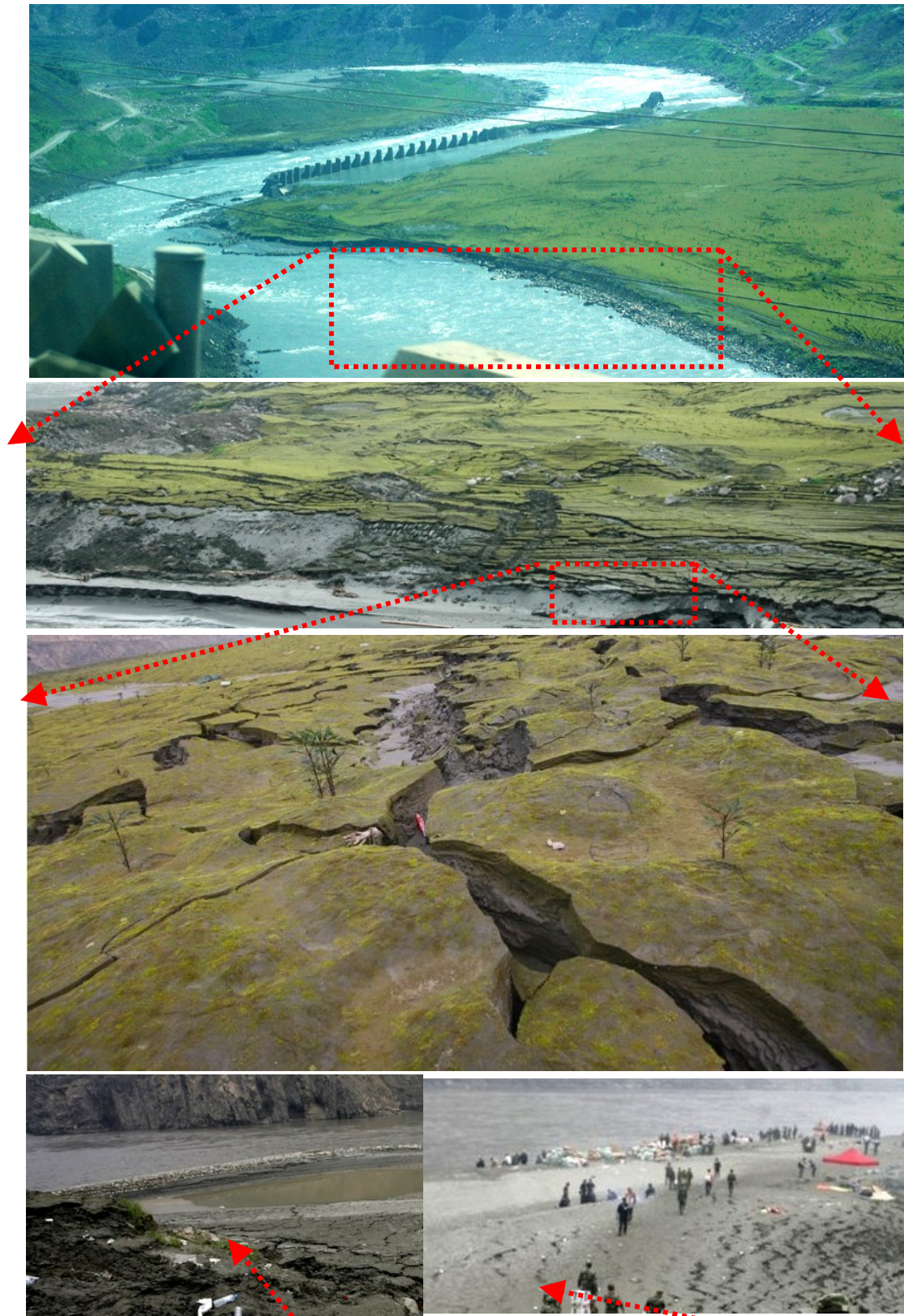


Figure 9.2. Effects of ground liquefaction and lateral spreading in the vicinity of Yingxiu of WenchuanCounty



Figure 9.3. Sandboils and surface ruptures in Qingchuan County



Figure 9.4. Lateral spreading of ground in the vicinity of Shoujiang Bridge



Figure 9.5. Sand boil in a school yard

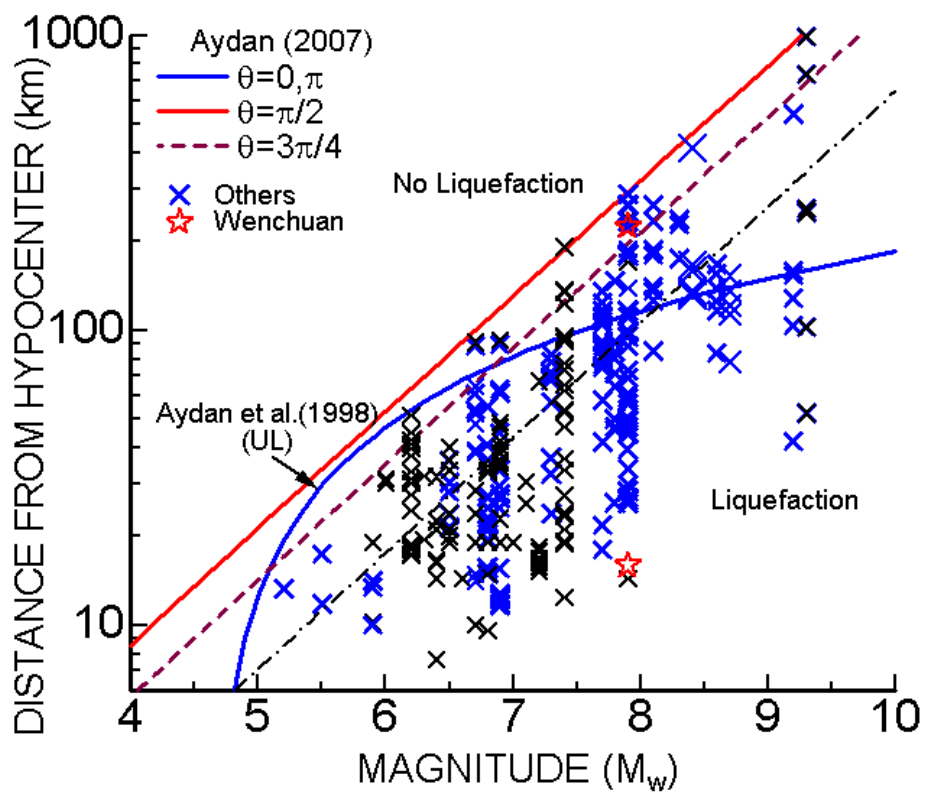


Figure 9.6. A comparison of wenchuan earthquake data with those of other earthquakes

11. DAMAGE TO BUILDINGS

This section is concerned with damage to buildings of various type. Buildings may be defined as

- a) Masonry buildings
- b) Timber framed buildings
- c) Reinforced concrete buildings.

Reinforced concrete buildings may be also sub-divided into pre-cast reinforced concrete buildings and cast-in-place reinforced concrete buildings.

11.1 Damage to Masonry Buildings (Adobe, Brick Masonry, Stone masonry)

Masonry buildings are generally common in rural areas and villages. Adobe type masonry buildings were generally observed in Qingchuan County. These simple buildings failed in out-of-plane mode (Figure 11.1). Furthermore, they have series damage at corners.



Figure 11.1. Damaged or totally collapsed adobe buildings

Stone masonry buildings are generally found in mountainous Aba region. Rocks used are sandstone, slate or limestone blocks. There are also some historical castles, which was built more than 1000 years ago and it was partially damaged by the 1933 Songpan earthquake. The 2008 Wenchuan earthquake damaged the same castle again. It was also reported that the damage in the vicinity of Taoping village, which is a touristic spot as the cultural village of Qiang people with a history more than 2000 years, is relatively small. Nevertheless, some houses were collapsed (Figure 11.2). There are also some watchtowers in the village. The top part of this watch towers was partially collapsed during this earthquake.

Wooden framed buildings were also observed in Qingchuan County, It is well known that the wooden houses generally performs well during earthquakes. The damage to wooden building generally occurs at the foundations and infill walls. Figure 11.3 shows an example observed in Qingchuan County. The foundation wall was made of stones with mud mortar. This wall toppled during earthquake. Furthermore, infill wall at other side of the building also toppled. Since other walls were intact, one may easily infer the directivity effect of the ground motion at this location. The direction of the collapse was perpendicular to the strike of the earthquake fault.



Figure 11.2. Damaged stone masonry buildings in Taoping village in Aba region



Figure 11.3. Toppled walls of a wooden framed house in Xiao village in Qingchuan



Figure 11.4. Damage to brick masonry buildings in the epicentral area

Brick masonry buildings are common in the epicentral area, particularly in Dujiangyan, Hanwang, Hongbai, Deyang, Jianyou etc. Most of single or two story buildings constructed as a brick masonry. The bricks are generally solid. Nevertheless, the recent bricks are hollowed. Typical dimensions of the bricks are 20cm long, 10cm wide and 5 cm thick. Most of brick houses have reinforced concrete slabs at each floor level. The damage to these buildings were due to out-of-plane failure. Furthermore, the damage was heavy at corners where walls interact with each other. These locations are prone to failure during high ground motions. However, some four-five story bricks buildings built in the same also exist. Figure 11.4 shows two examples of such building damaged by the earthquake. It is also noted that some walls failed in due to toppling while other walls are sheared. This once again indicates the directivity effect of the ground motions.

11.2 Reinforced Concrete (RC) Buildings

The reinforced concrete structures are the most commonly found buildings with four to six stories. The ground floor of this building are generally used shops, offices and storage rooms. They are framed structures with integrated or non-integrated in-fill walls. The reinforcing bars are generally smooth and infill walls are built with red-burned solid or hollow clay bricks using mortar. The floor height in the region is about 3 m. The reinforced buildings in the epicentral area were designed according to the lateral seismic intensity coefficient of 0.1 to 0.2g. The reinforced concrete buildings were built as either cast-in-place reinforced concrete building or pre-cast reinforced concrete building. The inspections of the reinforced concrete buildings indicated that they are mainly failed in the pancake mode. The concrete buildings having 3 or less stories were either slightly damaged or non-damaged.

The main causes of the collapse or heavily damage of the structures in this earthquake are different from those in other countries and can be broadly classified as follows:

- a. Poor concrete quality and workmanship,
- b. Plastic hinge development at the beam-column joints,
- c. Lack of shear reinforcement and confinement,
- d. Soft (weak) story,
- e. Pounding and torsion
- f. Fragile structural walls and lack of lateral stiffness,
- g. Soft ground conditions
- h. Landslides

- i. Permanent ground deformations due to faulting
- j. Ground motion characteristics (i.e. multiple shocks, long duration etc.).

Other features of damage to each type of reinforced concrete buildings will be explained separately. Furthermore, some landslide and faulting induced damage to reinforced concrete structures will be explained in this section.

(a) Cast-in place Reinforced Concrete Buildings

Figures 11.5 to 11.8 show some examples of heavily damaged or totally collapsed cast-in-place reinforced concrete buildings associated with some causes listed above. Although the earthquake mostly damaged these buildings, they performed much better than the pre-cast reinforced concrete buildings. They were more ductile. The collapse of these buildings occurred at ground floor due to soft-floor problem mainly. Since the building stands mainly on columns, the quality of the workmanship on beam-column joints and the concrete itself become of paramount importance. There were many examples of inadequate spacing of stirrups, insufficient and small diameter of bars. The use of hollow bricks considerably reduces the weight of the building. Nevertheless, they are more fragile and fail in a brittle manner. The infill walls are constructed as brick falls and they act as a shear wall upon the plastic hinging at column-beam joints. Due to the fragility of the infill walls, the resistance of the infill walls were expected to be none during the response of these buildings against strong motions induced by the 2008 Wenchuan earthquake. There are also some high-rise buildings particularly in Chengdu. These building were almost non-damaged during this earthquake. Since the ground motions in Chengdu was small during the Wenchuan earthquake, the structural seismic resistance of such building must be checked by considering nearby earthquakes such as on Dayi fault.



(a) Beichuan



(b) Beichuan



(c) Dujiangyan

Figure 11.5. Several examples of collapsed cast-in-place reinforced concrete buildings due to soft (weak) floor problem



Figure 11.6. Several examples of plastic hinge development at the beam-column joints, due to lack of shear reinforcement and confinement



Beichuan



Yingxiu

Figure 11.7. Several examples of damage to reinforced building due to soft ground conditions



(a) Thin bars



(b) poor granulometry

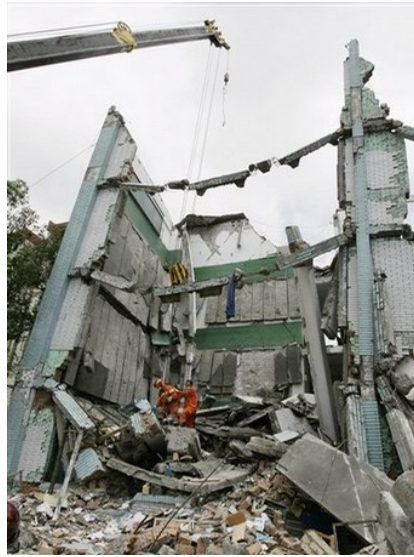
Figure 11.8. Construction quality problems



Figure 11.9. Damage due to pounding of adjacent buildings

(b) Pre-cast Reinforced Concrete Buildings

Most of casualties occurred due to the total collapse of the pre-cast reinforced concrete building constructed as residential buildings and school buildings (Figures 11.10 and 11.11). These buildings collapsed due to insufficient lateral resistance against the strong ground motions. The lateral beams with insufficient resistance failed at the column-beam connections. The lack of sufficient reinforcing bars and structural rigidity, these buildings dilapidated like LEGO houses. The all stories of the buildings piled up in a pan-cake fashion. These buildings were built undoubtedly in a short period of time. The technique of construction was probably imported from a country or countries without any major seismicity.



(a) Dujiangyan



(b) Ronghua-Shifang



(c) Mianzhu



(d) Hanwang

Figure 11.10. Collapsed pre-cast reinforced concrete buildings at various places



(e) Qingchuan



(f) Beichuan



(g) Yingxiu

Figure 11.11. Collapsed pre-cast reinforced concrete buildings at various places

11.3 Fault-Induced Damage to Buildings

The earthquake fault, known as Yingxiu-Beichuan fault started to rupture in the west of Yingxiu, passed through Beichuan and extended to Qingchuan County. Yingxiu and Beichuan town are situated just above the earthquake fault. The fault splays into numerous surface ruptures when it closes to the ground surface due to vertical stress reduction. Some surface ruptures measured in Yingxiu, Beichuan and Qingchuan are more than 2-3m. The permanent ground displacement as well as individual surface ruptures causes topographic changes and impose forced displacements on the surface and underground structures. Many buildings as well as other structures were damaged or totally collapsed due to these forced displacements induced by faulting (Figures 11.11. to 11.14). In spite of some damage some structures survived these displacements and deserve further detailed studies.



Figure 11.11. Damage to structures due to forced displacements induced by faulting in Beichuan



Figure 11.13. Damage to structures due to forced displacements induced by faulting in Yingxiu



Figure 11.14. Damage to structures due to forced displacements induced by faulting in Qingchuan

11.4 Landslide and Rock-fall Induced Damage to Buildings

This earthquake caused many slope failures resulting in large-scale failures called landslides. Such landslides were observed particularly in mountainous area and the hanging-wall side of the earthquake fault. Among all large-scale landslides, the landslides in Beichuan destroyed town and the landslides came from both mountains adjacent the town. The NW facing slope caused by mainly the sliding of limestone formation, while the SE facing slope was caused by the sliding along bedding plane and shearing of the phyllite-like layers (some referred it as mudstone???) (Figures 11.15 and 11.16). Another landslide at Donghekou destroyed the entire village. These scale landslides induced damage on buildings of a town are very rare and deserve further studies.

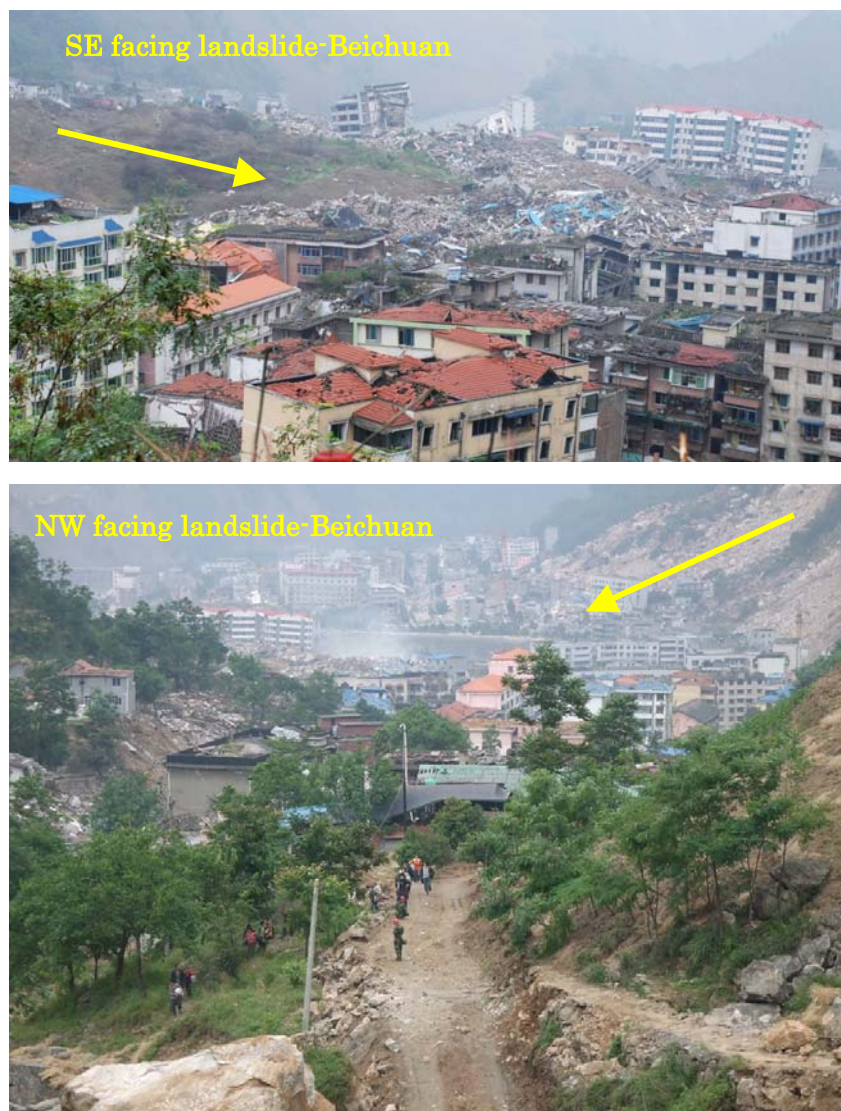


Figure 11.15. Views of the landslides in Beichuan



Figure 11.16. A close-up view of the NW-facing landslide in Beichuan

Rockfalls induced by ground shaking also caused damage in many places in the mountainous area. Figure 11.17 shows several examples of such damaged. Their impact may be of a large scale and the damage induced in residential buildings can be particularly of great concern. Especially, the question will be how to identify such blocks, which may be put into motion during earthquakes.

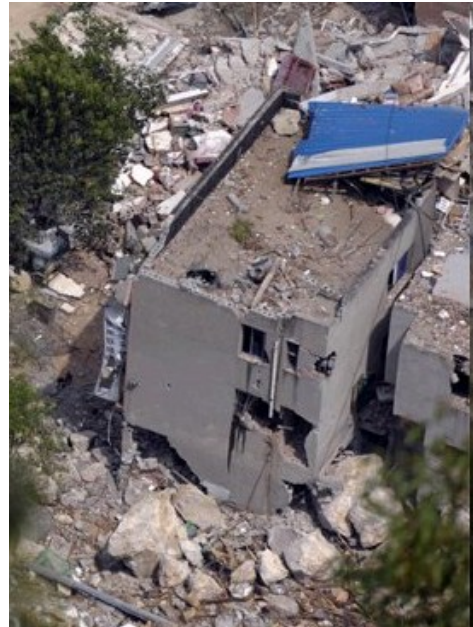


Figure 11.17. Rock fall induced damage on buildings

12 CONCLUSIONS

The 2008 Great Wenchuan earthquake in Sichuan Province of China caused the failure of natural slopes as well as cut-slopes besides the extensive damage to buildings, infrastructures and the loss of lives of more than 79000 people. The scale of slopes failures was tremendous and they indicated the vulnerability of natural slopes against failure during earthquakes, which are stable under non-seismic conditions. This topic probably deserves further studies and it implies the necessity of developing susceptibility maps of natural rock slopes against failure during earthquakes together with the consideration of discontinuous nature of rock mass. In addition, there were numerous rockfalls causing heavy casualties and damage in transportation system as well as buildings. Although it is a difficult topic to be dealt with, it is an urgent issue to be studied and addressed. If it is possible, rockbolts, rockanchors with wire meshes and shotcrete could be utilized to stabilize the disturbed slopes in the earthquake-affected area. Figure 9.12 may serve as a guideline for local engineers how to select the slope-cutting angle in actual restoration of the failed slopes. The so-called quake-lakes have a high potential to cause secondary disasters following the earthquakes by breaching or slippage due to piping. When their scales are so large as in the case of Tangjiashan quake-lake, the successful drainage or sustaining their stability by the construction of spillways are not easy issues to be dealt with. Nevertheless, the quake-lakes caused by the 2008 Wenchuan earthquake were successfully drained through the utilization various techniques together with software measures such as evacuation people to higher ground in spite of several unsuccessful hardware attempts. The Wenchuan earthquake also showed that underground structures, especially tunnels, are vulnerable to sever damage when they are constructed in active fault zones. If the linings could not accommodate the deformation, there may be collapses of non-reinforced concrete linings. In such zones, the linings must be constructed as reinforced. As for existing non-reinforced tunnel linings in active fault zones, some counter-measures must be introduced to retrofit it with steel platens or fiber-reinforced polymers with rockbolts.

REFERENCES

- Aydan, Ö. (2006): Strong motions, ground liquefaction and slope instabilities caused by Kashmir Earthquake of October 8, 2005 and their effects on settlements and buildings. Bulletin of Engineering Geology. No. 23(15-34).

- Aydan, Ö. and Hamada M. (2006): Damage to Civil Engineering Structures by Oct. 8, 2005 Kashmir Earthquake and Recommendations for Recovery and Reconstruction . Journal of Disaster Research, Vol.1, No.3 pp. 1-9.
- Aydan, Ö., Ohta, Y. (2006). The characteristics of ground motions in the neighbourhood of earthquake faults and their evaluation. Symposium on the Records and Issues of Recent Great Earthquakes in Japan and Overseas, EEC-JSCE, Tokyo, 114-120
- Aydan, Ö., T. Kyoya, Y. Ichikawa, T. Kawamoto and Y. Shimizu (1989). A model study on failure modes and mechanisms of slopes in discontinuous rock mass. *The 24th Annual meetings of Soil Mechanics and Foundation Eng. of Japan*, Miyazaki, 415, 1089-1093.
- Aydan, Ö., Sakoda, S. and Kumsar, H. 2006a. Stability of slopes under dynamic loading and its modelling. Symposium on Modern Applications of Engineering Geology, Turkish National Group of Engineering, Denizli, 101-109
- Aydan, Ö., Daido, M., Ito, T., Tano, H. and Kawamoto, T. (2006b): Prediction of post-failure motions of rock slopes induced by earthquakes. 4th Asian Rock Mechanics Symposium, Singapore, Paper No. A0356 (on CD).
- Burchfiel, B. C., Z. Chen, Y. Liu, and L. H. Royden (1995): Tectonics of the Longmenshan and adjacent regions, *Int. Geol. Rev.*, 37, 661– 735.
- China Earthquake Data Center (2008): A quick report on the strong motion data of 5.12 Wenchuan earthquake (in Chinese). <http://www.smsd-iem.net.cn/>
- China Geographical Survey Institute (2008): Tangjiashan quake lake (in Chinese). <http://www.cgsi.cn/>
- China Water Resources (2008): A series of reports on water level variations on Tangjiashan quake-lake (in Chinese). <http://www.cwr.cn/>
- Densmore, A. L., M. A. Ellis, Y. Li, R. Zhou, G. S. Hancock, and N. J. Richardson (2007): Active tectonics of the Beichuan and Pengguan faults at the eastern margin of the Tibetan Plateau, *Tectonics*, 26, TC4005, doi:10.1029/2006TC001987.
- Hamada, M. and Aydan, Ö. (2008): The 2008 Sichuan Great Earthquake Disaster and Technological Restoration and Recovery Support Activities of Interdisciplinary Liaison Council led by JSCE. WFEO-JFES-JSCE Joint International Symp. On Disaster Risk Management, Sendai, 12-25.
- HARVARD (2008): HARVARD Centroid Moment Tensor, Department of Earth and Planetary Sciences, HARVARD University, Cambridge, MA, USA.
- IGP-CEA (2008): Institute of Geophysics, China Earthquake Administration, M8 Wenchuan Earthquake. <http://www.cea-igp.ac.cn/index.htm>
- Kumsar, H., Aydan, Ö. and Ulusay, R. (2000): Dynamic and static stability of rock

- slopes against wedge failures. *Rock Mechanics and Rock Engineering*, Vol.33, No.1, 31-51.
- Lin, C.J. and Chai, J.F. (2008): Reconnaissance report on the China Wenchuan Earthquake May 12, 2008. *NCREE Newsletter* Vol. 3, No.3, Sep. 2008.
- Lu, Jun., Shunzhang Xue, Fuye Qian, Yulin Zhao, Huaping Guan, Xianjin Mao, Aiguo Ruan, Surong Yu, Wujun Xiao (2004): Unexpected changes in resistivity monitoring for earthquakes of the Longmenshan in Sichuan, China, with a fixed Schlumberger sounding array. *Physics of the Earth and Planetary Interiors* 145 (2004) 87–97
- Nishimura and Yagi (2008): Mega earthquake of May 12, 2008 in Sichuan province (in Japanese). http://www.geol.tsukuba.ac.jp/press_HP/yagi/EQ/20080512/
- Şengör, A.M.C. (1984). The Cimmeride Orogenic System and the Tectonics of Eurasia *Geological Society of America Special Paper*, 195, 1-82.
- Shimizu, Y., Ö. Aydan, Y. Ichikawa, T. Kawamoto (1988). An experimental study on the seismic behaviour of discontinuous rock slopes (in Japanese). *The 42nd Annual Meeting of Japan Society of Civil Engineers*, **III-180**, 386-387.
- USGS: U.S. Geological Survey, National Earthquake Information Center, Golden, CO, USA. <http://earthquake.usgs.gov/>
- Yamanaka, Y. (2008): May 12, 2008 Sichuan Earthquake, No.8 (in Japanese) http://www.seis.nagoya-u.ac.jp/sanchu/Seismo_Note/2008/NGY8.html
- Yang, Z.X., F. Waldhauser, Y.T. Chen and P.G. Richards (2005): Double-difference relocation of earthquakes in central-western China, 1992–1999. *Journal of Seismology* (2005) 9: 241–264.
- UNOSAT (2008): Overview of Tangjiashan quake lake, Beichuan, China from 3-8 June 2008. EQ-2008-000062-CHN. <http://www.unosat.org/>
- Xinhuanet (2008): Pictures of 5.12 Wenchuan earthquake. <http://www.xinhuanet.com/>